Biogeochemistry (2025) 168:75
https://doi.org/10.1007/s10533-025-01266-z

Effects of rooting, temperature, and organic horizon development on temperate forest soil carbon, nitrogen, and inorganic nutrients in transplanted soils

Justin B. Richardson · **Annise M. Dobson**

Received: 25 August 2024 / Accepted: 25 August 2025

Abstract Complex interactions controlling carbon (C), nitrogen (N), and inorganic nutrients: calcium (Ca), magnesium (Mg), potassium (K), phosphorus (P), in forest soils are difficult to tease apart due to covarying factors (e.g., soil parent material) and reductionist approaches can miss potential synergistic effects. We evaluated if increasing mean annual temperature (MAT), decreased organic horizon development, shallow tree rooting, and accumulation of C, N, and inorganic nutrients. We transplanted 144 mineral soil columns across six temperate forests from Virginia to New Hampshire and collected them 1-year and 4-years later. Our results show that organic horizon C, N, and nutrient pools were negatively associated with MAT with 4×to 5×greater pools at the coldest sites than the warmest sites. Since five-years of inputs from litterfall and throughfall monitoring show similar or increasing fluxes with MAT, differences were likely due to faster mineralization and transport from the columns. Transplanted mineral soil C, N, Ca, and P pools did not vary with MAT nor with root-access or root biomass, showing roots and organic horizon masses did not have consistent effects. Mineral soil root and MAT effects may still be developing or impacted by other variables not evaluated. Lastly, we found increases of organic phase Ca, Mg, K, and P from Year 0 to Year 1in the mineral soil across all six sites using Scanning Electron Microscopy- Energy-Dispersive X-ray Spectroscopy (SEM–EDS) imaging but only a significant effect of MAT or root-access for K. Our study highlights that MAT, organic horizon development, and nutrient accumulation and storage are linked but not in the mineral soil.

Keywords Nutrient cycling · Biogeochemistry · Forest floor · Nutrient sequestration · Temperate forest

Responsible Editor: Stephen D. Sebestyen

Supplementary Information The online version contains supplementary material available at https://doi.org/10.1007/s10533-025-01266-z.

J. B. Richardson (✉)
Department of Environmental Sciences, University of Virginia, Charlottesville, VA 22903, USA
e-mail: Justin.Richardson@virginia.edu

J. B. Richardson
Department of Geosciences, University of Massachusetts Amherst, Amherst, MA 01003, USA

A. M. Dobson
School of the Environment, Yale University, New Haven, CT 06511, USA

Introduction

The complex interactions controlling C, N, and nutrients (e.g., Ca, Mg, K, P) in the tree-soil system have been difficult to tease apart due to interdependent drivers and overlapping effects from trees and soil processes. Many of the common techniques used

Published online: 13 September 2025

to examine the tree-soil system are often spatially-limited (e.g., one forest), species-specific (e.g., one genera or species), reductionist approaches such as long-term forest treatment blocks (see Pretzsch et al 2019), laboratory growth chamber experiments (e.g., Medhurst et al 2006), and column experiments (e.g., Schindlbacher et al 2004; Street et al. 2023). While these techniques are useful for examining the effect of specific variables and limiting noise produced by non-target variables, these approaches are not able to capture interdependent drivers and potential synergistic effects. In particular, leaf litter production and organic horizon development may generate a mineral soil microenvironment that alters how trees develop shallow roots, the storage of inorganic nutrients, and soil organismal decomposition (McClaugherty et al 1985; Kooijman et al 2019; Gao et al 2021; Heděnec et al 2023; Bowden et al 2024). Altering or separating these intrinsically linked processes may influence the other components of the surface soil system. Here, we seek to examine the effects of climate (specifically temperature) and tree-controlled variables (e.g., litterfall, organic horizons, roots) on the biogeochemistry of C, N, and nutrients in a controlled upper mineral soil in temperate forests.

Mean annual temperature (MAT) is one of the dominant factors controlling many forest soil processes in temperate forests, specifically on biogeochemistry of elemental cycling (e.g., Adams et al 2019; Jelinski et al 2023) and surface soil development and tree rooting (e.g., Gao et al 2021; Zhang et al 2024). In the tree-soil system, warmer MAT promotes longer growing seasons and aboveground biomass production in temperate trees (Zani et al 2020) and allows for longer periods for decomposition by microorganisms and soil invertebrates (Rouifed et al 2010; Frouz et al 2015; Craig et al 2022). Increases in MAT may lead to net losses of soil organic carbon (SOC) within the organic horizon (combined Oi, Oe, Oa horizons) or upper mineral soil due to faster mineralization of litter-derived or root-derived SOC (Gao et al 2021; Bowden et al 2024). Tree genera can impact the quantity of annual litter inputs and litter quality such as C, N, and nutrient content of the litter (McClaugherty et al 1985; Richardson and Friedland 2016; Ott and Watmough 2021; Heděnec et al 2023). Subsequently, increased mineralization of SOC due to higher temperatures and oligotrophic-adapted tree genera can decrease storage of inorganic nutrients such as P, K, Ca, Mg (Augusto et al 2002; Hobbie 2015). Thus, quantifying nutrient cycling linkages with increasing MAT are needed to predict the long-term impacts on sustainability of natural and managed temperate forest ecosystems from climate change.

In addition to MAT, another key controller of surface soil processes is the actions of trees via leaf litter. Leaf litterfall from the canopy and understory accumulates on the surface of the soil, creating the organic horizon if inputs exceed decomposition and mineralization. The organic horizons are a dynamic reservoir for C, N, and inorganic nutrients and serve as sources for plant uptake or downward translocation to upper mineral soils (A horizons). It must be noted that higher inorganic nutrient content of litter has been linked to faster decomposition, in which litter chemistry such as higher N and Ca improves substrate quality for decomposition (Berg and McClaugherty 2020). Furthermore, litter decomposition via abiotic and microbially-mediated decomposition pathways can create more organic acids or mineral-associated organic matter (MAOM) compared to invertebrates that generate more particulate organic matter (POM) (Augusto et al 2002; Frouz et al 2015; O'Donnell et al. 2016; Kooijman et al 2019; Prescott and Vesterdal 2021). Changes in temperature and moisture can shift organic matter decomposition, organic horizon development, and organic acid releases (e.g., Küsel and Drake 1998; Qiu et al 2018; Wu et al. 2021), which can alter chemical weathering in the underlying mineral soil. Organic horizon development is generally promoted by greater litter inputs, lower litter quality, slower decomposition rates by invertebrates and microbial communities, greater hydric soil conditions, and concave soil surface topography (Kooijman et al 2019; Prescott and Vesterdal 2021). Lastly, green leaves alter the chemistry of precipitation during the growing season due to foliar leaching adding soluble C, N, and inorganic nutrients into rainfall (Van Stan et al 2012; Zhao et al 2023).

Tree roots play important roles in the cycling of C, N, and inorganic nutrients in temperate forest soils by enhancing available pools through rhizosphere interactions with mineral surfaces or enhancing loss of elements through root uptake. Live roots can alter the physical and chemical properties of soils creating the rhizosphere, the soil immediately adjacent to the root surface. The rhizosphere has higher DOC

concentrations, higher acidity, greater microbial biomass, and higher mineral dissolution rates than the bulk mineral soil (Séguin et al 2005; Liu et al 2022). The presence of live roots and their derived compounds (exudates and root litter) can serve the mechanism of 'priming', in which rhizodeposition promotes SOC mineralization (see Zhu et al. 2014a; Dijkstra et al 2021; Wang et al 2021). The exudates from tree roots and the dissolved organic acids from the organic horizon can also dissolve nutrients from minerals and that may leach deeper into the soil (Jones and Brassington 1998; Liu et al 2022). Lastly, roots also remove inorganic nutrients, particularly plant exchangeable and soluble forms, from soils as part of their uptake to sustain aboveground mineral nutritional needs (e.g., Hagen-Thorn et al 2004).

A major limitation to understanding temperature and tree effects on soil processes at landscape and regional scales is the wide variation in soil materials. Different particle sizes and proportions of minerals create heterogeneous responses in C and nutrient accumulation patterns in soils. Increased surface area with greater clay-sized particles, including clay minerals, aluminum (Al) and iron (Fe) oxyhydroxides, amorphous silicon (Si) forms promote the formation of organo-mineral complexes (Rasmussen et al 2018; Lang et al 2023; Wu et al 2025). Clay-sized particles can increase inorganic nutrient sorption and SOC retention rates due to their higher surface areas and greater charge density (e.g., Rasmussen et al 2018; Kome et al 2019; Lang et al 2023; Wu et al 2025). Conversely, larger sand-size particles have comparatively less surface area and greater porosity (e.g., Ouchiyama and Tanaka 1986; Scott et al 1996; Huang and Hartemink 2020), diffusion of air and moisture (e.g., Chauhan et al 2008; Neira et al 2015), and lead to lower sequestration of C (Scott et al 1996; Rasmussen et al 2018; Huang and Hartemink 2020) and inorganic nutrients (Šimanský, et al 2019). The abundance of slow weathering, nutrient poor aluminosilicate minerals (e.g., quartz and feldspars; Eberl 2004, Martín-García et al. 2015) compared with fast weathering, nutrient rich non-silicate minerals (e.g., carbonates; Wang et al 1999; Prietzel et al 2021) can alter the amount of inorganic nutrients sequestered in surface soils. Experiments utilizing homogeneous materials are needed to overcome the heterogeneity in soil materials and have been key to effective laboratory experimental designs (e.g., Scott et al 1996; Brandt et al 2014). Additional field-based experiments leveraging controlled soil media are essential to tease apart the complex interactions occurring in temperate forest soils.

The central goal of this study was to evaluate the synergistic influence of mean annual temperature (MAT), root presence, and organic horizon development on the accumulation of C, N, and inorganic nutrients in the organic horizon and mineral soil in secondary growth temperate forests along the Appalachian mountain range in the eastern US. To meet this objective, we transplanted in situ soil columns to eliminate parent material biases that typically limit comparability among soils and avoiding laboratory artifacts. In this study, we have investigated three main questions:

Question 1: Do transplanted soil columns in temperate forest with higher MAT have lower C, N, and inorganic nutrient accumulation rates in the organic horizon and mineral soil?

We expected lower C and inorganic nutrient accumulation in the organic horizon and mineral soil in transplanted soils at sites with higher MAT due to greater litter mineralization and lower accumulation of organic horizon and mineral soil SOC. With the decreased SOC, we also expected a subsequent decrease in sorption and retention of inorganic nutrients within the soil material. Lastly, we expected increased organic horizon development to correspond with a decrease in mineral soil accumulation of C, N, and inorganic nutrients due to storage within the organic horizons.

Question 2: Do transplanted soil columns with greater root biomass promote greater stabilization of C, N, and nutrients?

We expected decreased root biomass within increasing MAT and we hypothesized this would decrease SOC and inorganic nutrient accumulation. Moreover, we expected a decreased root biomass within the transplanted soil columns to occur with higher MAT due to decreased nutrients stored within the organic horizons and shallow mineral soil.

Question 3: Does the form of inorganic nutrients in the transplanted soil remain similar or shift to lesser mineral associated and greater organic-particulate forms with higher MAT or greater root biomass?

We expect that through time, inorganic nutrients will be stored within organic phases as the soil develops from nearly all inorganic nutrients. Moreover,

we expected that the organic phase nutrients increase will correspond with higher MAT denoting a shift in the decomposition pathway from organo-mineral forming decomposition to particulate matter forming decomposition.

Overall, we hypothesized that higher mean annual temperature would decrease the synergistic actions of organic horizon development, shallow root growth, and C, N, and inorganic nutrient accumulation within the mineral soil. Our study is one of the first to couple homogenized soil material transplant study design with a biogeochemical budget to evaluate inputs and accumulation rates. Information from this study will help address the underlying effect of climate, specifically MAT, on the organic horizon and mineral soil storage and accumulation rates of C and inorganic nutrients in secondary temperate forests of the eastern US.

Materials and methods

Field study sites

In 2018, the set of field sites was established to investigate temperature-driven variation in soil biogeochemistry covering a 1100 km (7°) latitude gradient (Fig. 1; Table 1), which coincides with the projected 1–7 °C MAT increase over the next 100 years (e.g., Melillo et al. 2014). Sites were chosen for their similar mixed non-residuum soils, hardwood vegetation dominance, minimal active management for timber, and physiographic montane positioning with eastern aspect to compare processes that vary with climate. Sites with shallow water tables, floodplain soils, abundant pines or spruces, active or recent timber harvesting, or > 200 m or < 50 m from a road were avoided. We choose one 600 m^2 plot per site instead of multiple plots at each location to reduce effects from heterogeneity in soil native parent material, site history, geomorphic positioning, and drainage class and for logistical limitations. The sites were along the Taconic, White, and Green mountains of New England down to the Valley and Ridge province of Pennsylvania and Maryland, and the Blue Ridge in Virginia. Precautions were taken to ensure relatively similar forest age, management histories, and distance from urbanization. First, the mountain sites were state or privately-owned forests and land-use history

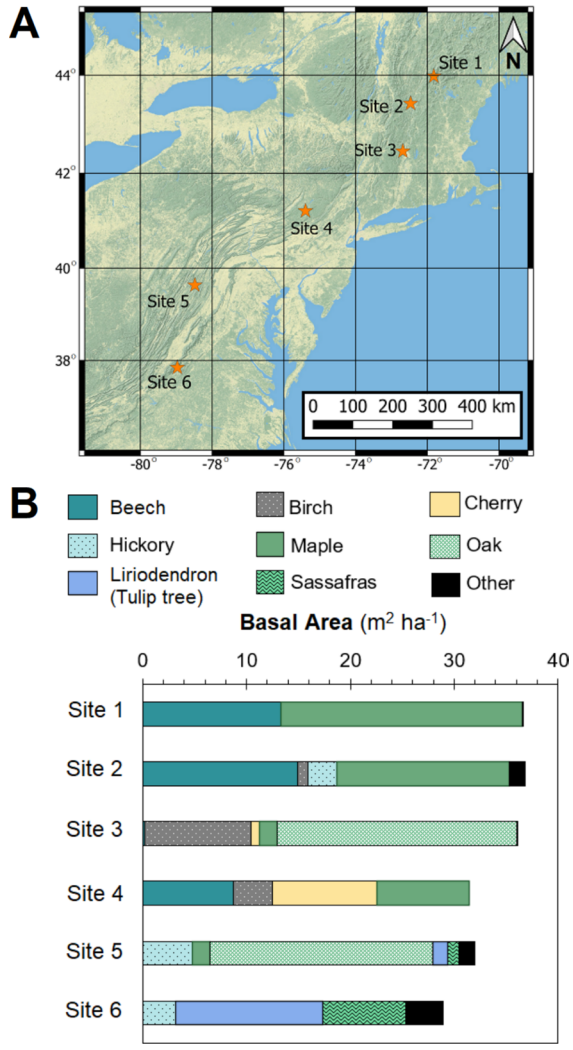

Fig. 1 **A** Location of sampling sites in orange stars. Green are forested land and mountain areas while yellow are low lying agricultural or developed areas. **B** Basal area of dominant tree genera and species across sites. Other includes white ash (*Fraxinus americana*), serviceberry (*Amelanchier arborea*), black walnut (*Juglans nigra*), eastern redbud (*Cercis canadensis*), and flowering dogwood (*Cornus florida*)

has determined their ages to be similar, 60–80 years of limited management following reforestation from clear-cutting or pasture.

Site 1 was situated on a terrace on Mt. Moosilauke in the White Mountains of New Hampshire while Site 2 was located on a foot slope of Mt. Ascutney, a monadnock mountain along the Vermont-New Hampshire border along the Connecticut River (Table 1). Site 3 at MacLeish Field Station (Zukswert 2013) was

Table 1 Field sites location, climate data, geologic, and soil data

Site #	Site Location	US State	Lat	Long	Elevation m a.s.l	30-yr MAT °C	30-yr MAP mm	Drainage class	In situ Soil
Site 1	Mt. Moosilauke	NH	43.9	− 71.8	570	6	1180	Well drained	Typic Dystrudepts
Site 2	Mt. Ascutney State forest	VT	43.4	− 72.4	380	6	965	somewhat excessively drained	Humic Dystrudepts
Site 3	MacLeish Field Station	MA	42.4	− 72.7	270	9	1205	Well drained	Typic Dystrudepts
Site 4	Tobyhanna State Forest	PA	41.2	− 75.4	610	8	1080	Moderately well drained	Aeric Fragiaquepts
Site 5	Green Ridge State Forest	MD	39.6	− 78.5	420	11	1066	Well drained	Typic Dystrudepts
Site 6	Lesesne State Forest	VA	37.8	− 78.9	380	14	1092	Well drained	Oxyaquic Hapludults

Climate data are 30 year normal annual averages from PRISM (PRISM Climate Group, 2023) and soil and geologic data are from SSURGO

set on top of a ridge, east of the Berkshire mountains in western Massachusetts (Table 1). The native soil at Site 1, Site 2, and Site 3 were dominated by young, glacial-till soils approximately 12 to 16 ka. Site 4 at Tobyhanna State Forest was set in the Poconos Mountains in Pennsylvania (Table 1), which had soils that were also young soil with an age approximately 12 ka, forming from periglacial alluvium near the southern edge of the Laurentide ice sheet (Ciolkosz et al., 1990). Site 5 in Green Ridge State Forest was at the shoulder slope position of a sandstone ridge in the Green Ridge mountains of western Maryland (Table 1). Lastly, Site 6 at Lesesne State Forest was situated on a foot slope in a raised valley on the Blue Ridge mountains of Virginia and was a deep, highly weathered soil (Table 1). The age has not been constrained due to colluvial inputs. All soils receive litterfall, have complete or partial organic horizon development, and are minimally managed with no nutrient fertilization nor biomass removal.

Trees within the 600-m^2 plot were identified and measured for DBH and basal area (Table 2). Northern hardwoods of American beech (*Fagus grandifolia*), birches (*Betula nigra*, *Betula papyrifera*, *Betula populifolia*), maples (*Acer saccharum* and *Acer rubrum*) were the dominant trees at Site 1, Site 2, Site 3, and Site 4 (Fig. 1), although white pine *(Pinus strobus*) and Eastern hemlock (*Tsuga canadensis*) were present in limited numbers and size. Site 5 and Site 6 were dominated by oak-hickory-tulip poplar (*Quercus rubrus* hybrids, *Carya* spp, and *Liriodendron tulipifera*) with interspersed red maple and American beech. Total basal area of the forests ranged between 28 and 37 m^2 ha^{-1}

Table 2 Field data collected from each site during the 2018–2022 experiment

Site #	Aboveground biomass kg m^{-2}	Basal area m^2 ha^{-1}	Mean annual Throughfall L m^{-2} yr^{-1}	Mean annual Litterfall g m^{-2} yr^{-1}	Organic horizon mass (Year 1) kg	Organic horizon mass (Year 4) kg
Site 1	32 ± 10	36 ± 13	1050 ± 160	503 ± 121	0.63 ± 0.05	1.53 ± 0.73
Site 2	40 ± 12	37 ± 11	1020 ± 150	472 ± 84	0.59 ± 0.11	1.41 ± 0.55
Site 3	23 ± 7	36 ± 9	1150 ± 190	612 ± 87	0.71 ± 0.12	0.86 ± 0.45
Site 4	21 ± 6	31 ± 7	710 ± 130	508 ± 78	0.30 ± 0.06	0.49 ± 0.29
Site 5	47 ± 14	30 ± 9	920 ± 240	524 ± 73	0.23 ± 0.06	0.46 ± 0.23
Site 6	26 ± 8	28 ± 7	1060 ± 230	469 ± 51	0.01 ± 0.00	0.20 ± 0.14

Field measurements of aboveground biomass are described in Sect. "Field study sites", litterfall collection is described in Sect. "Aboveground inputs of litterfall and throughfall"

(Table 2), which was comparable to maturing eastern hardwood forests basal area (McEvoy et al 1980; Keeton 2006). The basal area likely corresponds to varying age and maturation, with Site 1, Site 2, Site 3, and Site 5 approaching mature composition while Site 4 and Site 6 are mid-succession with early successional trees still present (e.g., cherry and sassafras). Furthermore, Site 6 was hit by a windstorm event that felled several large trees in 2019.

Forest composition was a key aspect of our study as it drives aboveground nutrient inputs via litterfall, root biomass, and many other genera specific ecophysiological functions. We aimed to limit variability by focusing on aggrading secondary forest regrowth and also representative, endemic forest composition of the region rather than search for limited or unique ecotones to keep tree genera constant. Because of this experimental approach to not control for tree genera, forest canopy size and genera composition differed between sites. American beech, maples, birches dominated the two most northern sites. For Site 1 and Site 2 forest basal areas, American beech and maple comprised 36–47% and 39–64%, respectively. Birch trees were important for Site 3, comprising 28% of the forest basal area. Hickory (pignut hickory *Carya glabra* and mockernut hickory *Carya tomentosa*), oak (Chestnut oak *Quercus montana*, southern red oak *Quercus falcata*, swamp white oak *Quercus abla*), and tulip tree dominated the two most southern sites. For Site 5 and Site 6 forest basal areas, hickory, oak, and tuliptree comprised 7–16%, 64–72%, and 5–49%, respectively. Sassafras (*Sassafras albidum*) was present at Site 5 and Site 6, comprising 5% and 12% of the forests basal area, respectively. Smaller, less abundant trees such as white ash (*Fraxinus americana*), serviceberry (*Amelanchier arborea*), black walnut (*Juglans nigra*), eastern redbud (*Cercis canadensis*), and Flowering dogwood (*Cornus florida*) were present and grouped together under 'Other' as they individually did not comprise > 5% of the forest basal area at any of the six sites. To capture the variability in basal area at each site, we divided the 600 m^2 plot into three equal subsections of 200 m^2 and calculated the standard deviation as the basal area among the three subsections. Standard deviation in aboveground biomass followed a similar process but using the estimated biomass for each tree.

Soil column deployment and collection

In October and November 2018, 24 soil columns were deployed at each of the six field sites. Soil columns were 7.6 cm in diameter and 12.7 cm in length and made from polyvinyl chloride (PVC). To hold the soil material in place, 1-mm fiberglass mesh was added to the bottom of the columns. We deployed 12 soil columns with root-access screened windows (two circular 20-cm^2 windows on opposing sides of the column, centered on the midpoint of the column length) of 1-mm fiberglass mesh and 12 root absent columns without root-access windows. The root-access windows were positioned below the surface of the soil to promote root access to the mineral soil and prevent overland flow into the column. Soil columns were filled with homogenized fine sand sized quartz-feldspar sediment deposited by Tropical Storm Irene in 2011. The sediments were washed to remove large organic matter and cleaned with four treatments of 5% hydrogen peroxide (H_2O_2) and 3% sodium hypochlorite (NaClO) over 24 h and three 18.2 MΩ deionized treatments to remove the Na^{+1} and ClO^{-1}. To add surface area for microsite formation, commercial kaolinite was added to increase the clay content to 10% by mass and homogenized by dry mixing. We chose kaolinite to increase the surface area but not add high surface charge that would alter inorganic nutrient sorption. Using a Rigaku Miniflex-2 and whole pattern profile fit module in PDXL2 (Rigaku corporation 2007–2017), the final mineralogy was determined to be 55% quartz, 20% albite, 8% mica (muscovite and biotite mix), 9% kaolinite, and 8% hornblende. Soil columns were buried 10 cm into the surface soil and filled with the soil mixture to the top of the soil horizon, which was approximately 0.57 kg for a bulk density of approximately 1.25 g cm^{-3}. Every year, germinated seedlings within the soil columns were clipped. The first round of soil columns were harvested after 1 year in 2019, including the newly formed organic horizon and its total mass (Table 2). The second round of soil columns were harvested in 2022, after 4 years of deployment, including the organic horizon (Table 2).

Aboveground inputs of litterfall and throughfall

Three litterfall traps were deployed at each of the six study sites. Litterfall traps are 1.2 m tall and

0.9 m × 0.9 m PVC pipe frames with plastic mesh to collect leaves and woody debris. Litterfall trap nets were repaired, replaced, or re-secured in May and June and emptied in October and November, with the varying window due to differences in leaf out and fall senescence timing along the climate gradient. Litterfall was separated by tree species or genera and total litterfall mass was determined. Since the twigs and branches were too large to fit into the soil columns, exhibited high variability, and undergo a different decomposition pathway than leaves due to their higher lignin content and variable contact with the soil surface (Pietsch et al 2014), woody debris was not included in the litterfall inputs to the soil columns.

Four throughfall collectors were deployed at each site to capture throughfall input into the soil columns. Throughfall collectors were acid washed 20-L vessels with a funnel (diameter = 10.2 cm) for collection extending from a sealed lid, secured with 4.5 kg weight to keep it vertical. Fiber glass mesh covered the funnel, preventing debris > 1 mm from entering. The throughfall collectors were emptied twice a year, once in April–May for winter throughfall and again in October and November for growing season throughfall. The total volume of throughfall collected was weighed in the field (Table 2) and one representative 1-L subsample from each collected (including settled and adhered particles) was filtered with a Whatman 1 filter. A 50 mL subsample was acidified with 5 mol L^{-1} hydrochloric acid (HCl) and stored for C and N analysis while the remaining solution was oxidized with H_2O_2, acidified with 15.8 mol L^{-1} nitric acid (HNO_3), was filtered < 0.2 µm, dried down to 50 mL in a fume hood at 100 °C and analyzed for inorganic element concentrations (Supplemental Table S1).

Throughfall, litterfall, organic horizon, and mineral soil chemical measurements

For solid phase total organic C and N measurement, 1.0 g subsample of the bulk soil was acidified with 2 mL of 1 mol L^{-1} HCl to remove any inorganic C (see Dhillon et al 2015). The subsample was then re-dried, ground with an agate mortar and pestle, passed through a 0.10 mm sieve. Next, 15 mg of the ground, acidified subsample was weighed and folded in tins and analyzed for C using a Costech Elemental Combustion System 4010 analyzer (Costech Analytical Tech Inc, Valencia, California, USA). Every 10 samples included a blank and two continuing calibration verification (CCV) materials, acetanilide and atropine. Recovery rates for CCV were 100.1% and coefficient of variation (CV) was 0.3%. Subsamples of throughfall were analyzed for dissolved organic carbon (DOC) and dissolved organic nitrogen (DON) using a Shimadzu TOCV with TNM module, which included blanks, duplicates, and spikes. Procedural blanks had DOC and DON below limit of detection, duplicates were < 3% CV, and spikes had 94 to 101% recovery rates.

Mineral soils were strong-acid digested for pseudototal concentrations following EPA Method 3050B, which is an optimal technique to measure all nutrients not within aluminosilicate minerals, including exchangeable, organically-bound, oxyhydroxide-bound, and precipitated forms of inorganic nutrients (see Chen and Ma 2001). Mineral soil concentrations are presented in Supplemental Table S3. First, 1.00 g of the mineral soil from each soil column was weighed into 50 mL centrifuge tubes acidified with 5 mL of trace metal grade reverse aqua regia (9:1 ratio of 15.3 mol L^{-1} HNO_3 to 12.1 mol L^{-1} HCl acid) and heated on a hotplate to 90 °C for 45 min. Soils were not ground to avoid creating fresh surfaces for dissolution of silicate minerals. With every 20 samples, a preparation blank, a duplicate, and a standard reference material (SRM) was included. Montana Soil 2711a and San Joaquin Soil 2709a from the National Institute of Standards and Technology (NIST, Gaithersburg, MD, USA) were used for QA/QC. The digestates were then diluted to 50 g using de-ionized water and a subsample was diluted further at 1:5 ratio for instrumental analysis.

Litterfall and organic horizon samples were ground to < 2 mm and a 1.00 g homogenized sample were ashed at 500 °C for 8 h to remove organic materials which reduce the efficiency of acid-based digestions. For litterfall samples, triplicate measurement at the species level for each site and each year was measured while the organic horizon consisted of the Oi and Oe materials within each soil column. The ash was then acidified with 5 mL of reverse aqua regia and heated at 90 °C for 45 min. With every 20 samples, a preparation blank, a duplicate, two SRMs NIST 1547a and NIST 1537a from the NIST were used for QA and QC. The digestate was diluted to 50 g with deionized water and further diluted 1:5 for analysis. Litterfall concentrations and organic horizon

concentrations are presented in Supplemental Fig. S1 and Supplemental Table S2, respectively.

For elemental analysis of mineral soil digests, organic horizon digests, and leaf litter digests for inorganic nutrient (Ca, K, Mg, P) concentrations we used an Inductively Coupled Plasma Optical Emission Spectrometer (ICP-OES) Agilent 5110 (Agilent Technology, Santa Clara, California, USA). Recoveries for pseudototal digests of soil Ca, K, Mg, and P were 83 – 107% of their certified values. The metal concentration coefficient of variation between intra-sample duplicates was < 6% and metal concentrations in the preparation blank samples were < 0.1% of their analyte concentrations.

Soil imaging and processing

Undisturbed miniprofiles (4.2 cm length, 2.1 cm width, 1.8 cm depth) were collected from the top of each soil column to image the stabilization of nutrients at the surface of the transplanted soil (see Stoops 2021 on methods for collection and preparation of soil thin-section). For 'Root present' soil columns, collection was aimed toward the window to ensure capturing intruding tree roots. Miniprofiles were frozen at − 80 °C, freeze-dried to remove moisture, and fixed with low viscosity (225–425 cPs at 23 °C) epoxy resin EPO-TEK 301-2 (Epoxy Technology, INC, Billerica, MA, USA). Miniprofiles were cut in the center along the lengthwise axis. Energy dispersive x-ray spectroscopy (EDS) was performed to identify elemental maps of Al, Si, Ca, Mg, K, and P across the miniprofiles and conducted with a beam current of 200.0 nA and voltage of 15 kV on a Zeiss Evo 50 scanning electron microscope.

The EDS element maps of the miniprofiles were processed using Matlab Image Processing App (Matlab R2023a, The Mathworks INC, Natick, MA, USA). For each element, images were converted to gray scale and then using Matlab Image Segmenter App, each EDS image was converted into binary maps of presence-no presence of each element. This technique has been applied to image soil organic matter (e.g., Sudarsan et al 2016) and texture and moisture content (Kaplan et al 2024). We utilized manually defined threshold count levels over the software defined global thresholds to better avoid over-inclusion from back noise and avoid under-inclusion of distinguishable nutrient-bearing organic matter with lower count rates. Using the binary EDS maps, we determined aluminosilicate phase nutrients (including nutrients within secondary Al and Si phases) as those co-occurring in the same pixel as Al and Si and organic-form nutrients as those independent of Al and Si. The pixels of the aluminosilicate phase nutrients and organic-form nutrients were summed and divided by their respective total binary pixel count to determine the proportion of aluminosilicate phase (%) and organic phase (%) Ca, Mg, K, and P within each of the 36 columns. Due to the use of an organic resin, C and N could not be imaged.

Descriptive and statistical analyses

Descriptive statistics as well as parametric and non-parametric statistical tests were calculated in Matlab R2023a. In text values either report minimum and maximum values; arithmetic mean values ± 1 standard error (SE) are presented in text and in figures.

We performed all model analysis using R version 4.4.0 (R Core Team 2024). Linear mixed-effects models (LMMs) were fitted using the lmer function from the lmerTest package (Kuznetsova et al 2017) to examine the relationships between MAT and nutrient pools in throughfall and litterfall (C, N, Ca, Mg, K, P). Site and litter trap replicate were included as random effects in all models to account for site-specific variability. For questions 1 and 2, we compared organic horizon, mineral soil pools, and root biomass in soil columns by root-access (mesh windows), MAT, and year using linear mixed effect models with site and column replicate nested within site as random effects. We ran additional models with root biomass in place of root-access but present root-access/exclusion models here as the results were similar and no variables differed in significance between two sets of models. For question 3, we compared the proportion of aluminosilicate phase (%) and organic phase (%) Ca, Mg, K, and P from the SEM–EDS analyses with MAT and root-access. For each LMM, we estimated p values using Satterthwaite's method in lmerTest (see Kuznetsova et al 2017). We tested the model assumptions of normality of residuals and homoscedasticity with residual versus fitted value plots, and evaluated model fit with marginal and conditional R^2 using function r.squaredGLMM in the MuMIn package (Barton 2023). In all cases we report standardized coefficients in tables. We plotted raw data alongside

model predictions generated with the ggpredict function from the ggeffects package (Lüdecke 2021). For brevity, we have reported LMM coefficient, standard error, t-value, and p-value results in the supplemental materials.

Organic horizon and mineral soil retention of aboveground inputs

To further examine organic horizon accumulation with respect to inputs, we calculated the retention of litterfall and throughfall-sourced C and nutrients using Eq. 1. In this equation, LF is litterfall, TF is throughfall, OH accumulation is the corresponding organic horizon pool accumulation rate. The goal of this simplistic equation is to evaluate the amount of C and nutrients stored within the organic horizon over 1 and 4 years of organic horizon development.

$$\frac{[OHaccumulation]}{[LFflux + TFflux]} = \%RetentionbyOrganichorizon \quad (1)$$

To examine if aboveground litterfall and throughfall were the key sources and retained within the mineral soil, we determined the ratio of the amount of C and nutrients inputs with the pool within the mineral soil using Eq. 2. In this equation, MS accumulation is the mineral soil accumulation rate for each elemental pool at each site. The goal of this simplistic equation was to evaluate if the amount of C and nutrients stored within the mineral soil that can be solely attributed to litterfall and throughfall and not stored in the organic horizon over 1 and 4 years of mineral soil development.

$$\frac{[LF + TF - OHaccumulation]}{[MSaccumulation]} = \%LF\&TFRetained \quad (2)$$

Results

Litterfall and throughfall C, N, and nutrient fluxes

The 2018–2022 litterfall collected by litterfall traps at the six sites (Table 2) were not significantly different using the Kruskal–Wallis test ($p = 0.19$), and litterfall across sites and years had an overall average (arithmetic mean) dry weight mass of 515 ± 82 g m^{-2} yr^{-1} and ranged from 469 to 612 g m^{-2} yr^{-1}. Genera-specific effects on litter C and N concentrations were not significant. Average litterfall C concentration was 479 ± 11 g kg^{-1} and average litterfall N concentration was 27 ± 2 g kg^{-1} (Supplemental Fig. S1). For Ca and Mg litterfall concentrations, hickory, tuliptree, and sassafras were significantly higher than the other genera (Supplemental Fig. S1). This trend of higher concentrations for hickory, tuliptree, and sassafras continued for K and P, but with fewer significant differences (Supplemental Fig. S1).

Annual litterfall C fluxes were generally comparable among the six sites for the five years with an average of 245 ± 32 g m^{-2} yr^{-1} (Supplemental Figure S2). Litterfall N fluxes also were generally comparable among the six sites for the five years with an average of 13.9 ± 1.8 g m^{-2} yr^{-1} (Supplemental Figure S2). Average litterfall fluxes were 6.1 ± 1.6 g m^{-2} yr^{-1} for Ca, 0.9 ± 0.3 g m^{-2} yr^{-1} for Mg, and were significantly different among the six sites using the Kruskal–Wallis test with post-hoc Wilcoxon rank sum test (Supplemental Figure S2). In particular, litterfall fluxes of Ca and Mg at Site 5 and Site 6 were significantly higher than average Site 1 and Site 4 (Supplemental Figure S2; $p < 0.05$). Average litterfall K fluxes were comparable among the six sites with an average of 1.28 ± 0.39 g m^{-2} yr^{-1}. Average litterfall P fluxes were 0.38 ± 0.12 g m^{-2} yr^{-1}significant ly higher for Site 2 and Site 6 than Site 1, Site 4, and Site 5 ($p < 0.05$), using the Kruskal–Wallis test with post-hoc Wilcoxon rank sum test (Supplemental Figure S2). Litterfall C, N, Ca, Mg, K, and P fluxes and litter mass fluxes were comparable with Ott and Watmough (2021) in Ontario CA, Gosz et al (1972) in New Hampshire at Hubbard Brook, and Muller and Martin (1983) in eastern Kentucky.

To determine if different litterfall fluxes across site were associated with temperature, we compared litterfall fluxes with MAT and across the 5-yr of collections using a LMM (see Sect. "Descriptive and statistical analyses" for description; Supplemental Table S4; Fig. 2). Litterfall fluxes of C, N, K, and P did not significantly vary with MAT. Litterfall fluxes of Ca and Mg significantly increased with MAT. There were significant differences among sampling years for C and all nutrients (Supplemental Table S4), noting that variability in precipitation patterns, extreme heat events, and other effects on the

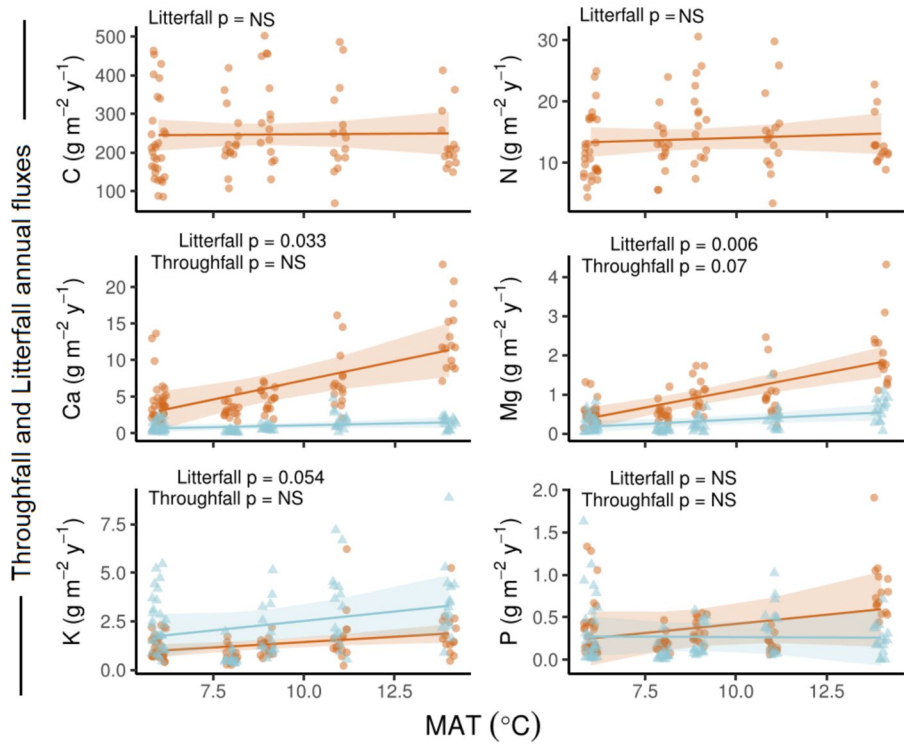

Fig. 2 Comparison of litterfall (orange circles) and throughfall (blue triangles) fluxes of C, N, and inorganic nutrients from the 6 sites across 5 years of collections with MAT from PRISM Climate Group (2023). Throughfall C and N was negligible compared to litterfall at < 1 g m^{-2} yr^{-1} for C and < 0.3 g m^{-2} yr^{-1} for N. The predictions are based on a linear mixed-effects model with random effects of trap nested within site. Continuous lines represent the model's predicted values, and 95% confidence intervals were calculated using the model's estimated variance. Symbols represent raw data. Full model results in Supplemental Tables 4 and 5, and random effects in Supplementary Table 9

intra-annual scale can alter litterfall mass with subsequent effects on C and nutrients.

Throughfall can be an important input of nutrients to forest soils and thus needed to be quantified to capture nutrients that can be added or sequestered in the organic horizon and mineral soil. Throughfall is distinctly different from bulk deposition, wet deposition, or dry deposition because it captures interactions with foliar surfaces and can leach nutrients from the leaves. Annual throughfall for the 5-yr collections ranged between 710 and 1150 L m^{-2} yr^{-1} (Table 2) and was generally comparable among sites, except Site 4 had significantly lower throughfall collected than Sites 1, 2, 3, and 6. Due to the significantly smaller mass of throughfall collected, throughfall fluxes for C, N, Ca, Mg, K, and P were significantly lower for Site 4 compared to the other sites using the Kruskal–Wallis test and post-hoc Wilcoxon Rank Sum test. Annual throughfall C fluxes had an overall average of 1.02 ± 0.17 g m^{-2} yr^{-1} and were not significantly different among the six sites, except Site 4. Annual throughfall N fluxes had an overall average of 0.19 ± 0.03 g m^{-2} yr^{-1} and were not significantly different among the six sites, except Site 4. Overall average throughfall fluxes were 1.06 ± 0.27 g m^{-2} yr^{-1} for Ca, 0.34 ± 0.09 g m^{-2} yr^{-1} for Mg, 2.49 ± 0.59 g m^{-2} yr^{-1} for K and 0.29 ± 0.11 g m^{-2} yr^{-1} for P (Supplemental Figure S2). Average throughfall Ca, Mg, and K fluxes at Site 5 and Site 6 were significantly higher than Site 1 and Site 4 using the Kruskal–Wallis test with post-hoc Wilcoxon rank sum test. Average litterfall P fluxes were significantly higher for Site 2 than Site 1, Site 4, and Site 6.

We compared throughfall fluxes with MAT at each site and across the 5-yr of collections using a LMM (see Sect. "Descriptive and statistical analyses" for description) to determine if there were relationships with temperature or time over the course of the 5-yr sampling period (Supplemental Table S5; Fig. 2). Throughfall fluxes of Ca, Mg, K, and P did not significantly vary with MAT. There were significant differences among sampling year for Ca, Mg, K, and P (Supplemental Table S5). However, since throughfall Ca, Mg, and K fluxes were greater at Site 5 and Site 6, our organic horizon and mineral soil evaluations include normalized comparisons to throughfall and litterfall.

Organic horizon development and elemental pools

The organic horizon is central to physical and chemical processes of the upper mineral soil and stores litterfall and throughfall added nutrients. All soil columns began without any forest floor coverage in summer of Year 0 (2018) and began formation with the autumnal litterfall of Year 0. Organic horizon masses in Year 1, one year after deployment, showed increases to an average of 0.41 ± 0.28 kg m^{-2}. By Year 4, organic horizon masses further increased across all sites to 0.82 ± 0.22 kg m^{-2} (Table 2 for site specific data). As part of our first hypothesis, we expected organic horizon development to decrease with increasing mean annual temperature. By Year 1, Site 5 and Site 6 organic horizons (0.009 ± 0.002 kg m^{-2} and 0.23 ± 0.06 kg m^{-2}, respectively) were significantly smaller than at Site 1, Site 2, and Site 3 (0.63 ± 0.05 kg m^{-2}, 0.59 ± 0.11 kg m^{-2}, and 0.71 ± 0.12 kg m^{-2}, respectively) using the Kruskal–Wallis Test with post-hoc Wilcoxon rank sum test ($p < 0.05$). Similarly in Year 4, Site 5 and Site 6 organic horizons (0.17 ± 0.02 kg m^{-2} and 0.47 ± 0.04 kg m^{-2}, respectively) were significantly smaller than Site 1, Site 2, and Site 3 organic horizons (1.53 ± 0.09 kg m^{-2}, 1.42 ± 0.19 kg m^{-2}, and 0.86 ± 0.08 kg m^{-2}, respectively) using the Kruskal–Wallis Test with post-hoc Wilcoxon rank sum test (Supplemental Figure S3, $p < 0.05$).

Central to question 1, we examined organic horizon C and nutrient pools with respect to MAT across the six sites, first using Kruskal–Wallis with post-hoc Wilcoxon rank sum test and second using a Linear Mixed-effect Model (see Sect. "Descriptive and statistical analyses"). From the Kruskal–Wallis test, organic horizon C, N, K, and P pools at Site 1 and Site 2 were consistently significantly higher than Site 5 and Site 6 in Year 1 and Year 4 (Supplemental Figure S3). Organic horizon Ca and Mg pools in Year 1 were similar across sites, except Site 6 which was significantly lower than all other sites ($p < 0.05$). By Year 4, Site 1 and Site 2 had significantly higher organic horizon Ca pools than Site 4 and Site 6 (Supplemental Figure S3). Using the LMM, we compared organic horizon C and nutrient pools within the year of collection as a categorical variable and MAT as a continuous variable across the six sites. Organic horizon pools of C, N, and inorganic nutrients we measured significantly decreased with MAT (Fig. 3, Supplemental Tables S6 and S11).

Organic horizon C, N, and nutrient accumulation and input retention

Using the changes in organic horizon concentrations and masses from Year 0, Year 1, and Year 4, we were able to estimate the rate of C and nutrient storage by the organic horizon along the climate gradient (Table 3). From Year 0 to Year 1, Site 1, Site 2, and Site 3 organic horizon accumulation rates of C, N, Mg, K, and P were significantly greater than Site 5 and Site 6 (Table 3). From Year 1 to Year 4, Site 1 and Site 2 organic horizon accumulation rates of C, N, Ca, Mg, K, and P were significantly greater than all other sites (Table 3). Furthermore, we compared Year 0 to Year 1 with Year 1 to Year 4 organic horizon accumulation rates, all sites significantly decreased, except Site 6 which significantly increased.

The results shown in Table 3 reveal that Site 1 through Site 4 had higher retention rates of C and nutrients than Sites 5 and Site 6. From Year 0 to Year 1, Site 1 and Site 2 had > 67% of the C and N while Site 5 and 6 retained 1–33% from the first litterfall of the previous year. From Year 0 to Year 1, Site 1 through Site 4 retention of Ca, Mg, and P exhibited a range of retention from 29 up to 99% of the added litterfall and throughfall inputs, which was greater than the 0.2 up to 30% for Sites 5 and Site 6. From Year 1 to 4, Site 1 and Site 2 had significantly higher retention rates of all C, N, Ca, Mg, and P than Site 3 through Site 6. Across the six sites and years collected, K had the lowest retention rate compared to the other elements but was still significantly greater for Sites 1 and 2 than Site 5 and Site 6.

Mineral soil C, N, and nutrient pools

Continuing with question 1, we sought to determine if transplanted mineral soil storage of C and nutrients increased with higher mean annual temperature. Our results primarily show site-specific differences but no trend across the temperature gradient. All transplanted mineral soil columns began with the same starting material in Year 0 (Supplemental Fig. S4). By Year 1, mineral soil C pools were significantly higher than starting at Year 0 and were lower for Site 1 (269 ± 22 g m^{-2}) compared to Site 5 (468 ± 47 g m^{-2}).

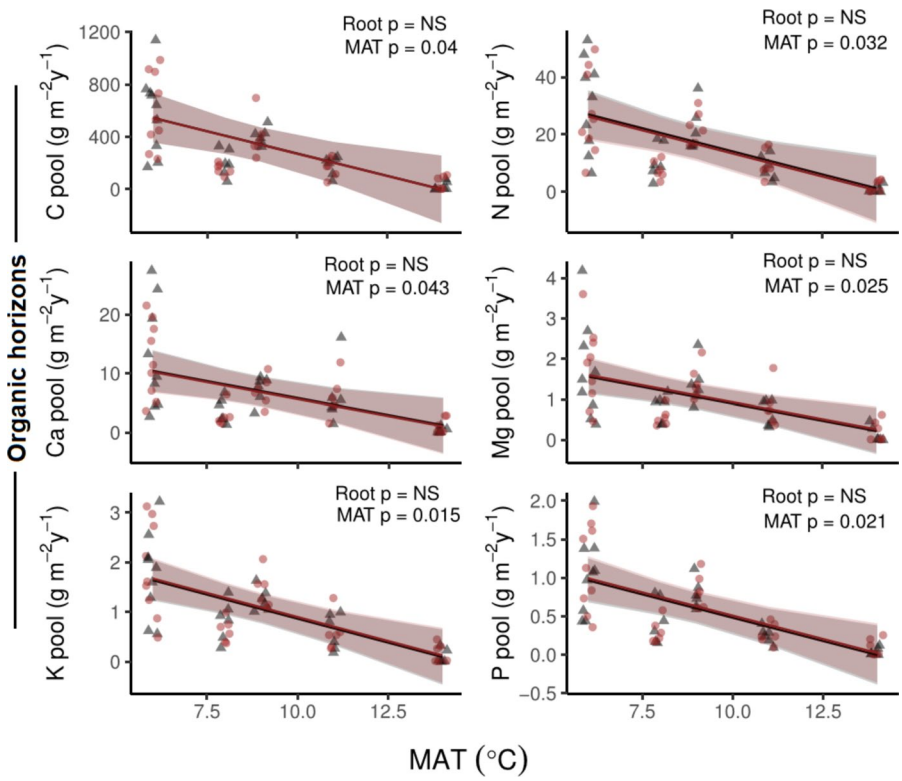

Fig. 3 Organic horizon C and nutrient (N, Ca, Mg, K, P) pools in the soil cores across MAT 30 year averagesand separated by root access (red) and root exclusion (black). The predictions are based on a linear mixed-effects model with random effects for replicates nested within site. Continuous lines represent the model's predicted values, and 95% confidence intervals were calculated using the model's estimated variance. Full model results are provided in Supplemental Table 6, random effects in Supplementary Table 9, and alternative models including root biomass in place of root access/exclusion in Supplemental Table 11

By Year 4, mineral soil C pools increased further and were significantly higher at Site 5 and Site 6 (2484 ± 37 and 2484 ± 47 g m^{-2}, respectively) than Site 1 and Site 2 (1684 ± 21 and 2123 ± 35 g m^{-2}, respectively). Similarly, mineral soil N pools at Site 5 and Site 6 (33 ± 3 and 26 ± 5 g m^{-2}) compared to the Site 1 through Site 4 (13 to 19 g m^{-2}). By Year 4, mineral soil N pools no longer exhibited a pattern along the gradient, with Site 2 and Site 5 (117 ± 17 and 144 ± 29 g m^{-2}, respectively) were significantly greater than the other sites (45 to 76 g m^{-2}).

Surprisingly, transplanted mineral soil Ca and P pools were not significantly different among the six sites in Year 1 (Ca was 84 to 103 mg m^{-2} and P was 16 to 20 mg m^{-2}, respectively) and in Year 4 (Ca was 98 to 111 mg m^{-2} and P was 21 to 26 mg m^{-2} respectively) in the soil columns (Supplemental Figure S4). Mineral soil Mg pools in the soil columns were not significantly different among the six sites in Year 1 (97 to 115 mg m^{-2}) but Site 2 and Site 5 attained significantly greater Mg pools (162 ± 10 and 175 ± 18 mg m^{-2} respectively) than Site 1 and Site 4 (120 ± 3 and 128 ± 4 mg m^{-2} respectively). Similarly, mineral soil K pools in the soil columns were not significantly different among the six sites in Year 1 (K was 31 to 50 mg m^{-2}) but Site 2 and Site 5 (85 ± 6 and 87 ± 10 mg m^{-2}, respectively) attained significantly greater K pools than Site 1 and Site 4 (162 ± 10 and 175 ± 18 mg m^{-2} respectively). However, the LMM revealed mineral soil Mg and K significantly decreased with increasing MAT, but Ca and P did not (Fig. 4, Supplemental Tables S7 and S12).

Using the changes in mineral soil from Year 0, Year 1 and Year 4, we were able to estimate the rate of C and nutrient accumulation in the mineral soil along the climate gradient (Table 4). Overall, there were no consistent trends in mineral soil C, N, and nutrient accumulation rates among the six sites. From Year 0 to Year 1 and Year 1 to Year 4, Site 1 and Site 3 mineral soil accumulation rates of C and N were significantly lower than Site 5 (Table 4). From Year 1 to Year 4, Site 1, Site 2, Site 4, and Site 5 mineral soil accumulation rates of C and N increased while Ca, K, and P decreased (Table 4).

Table 3 Organic horizon mean rate of accumulation rates of C, N, and inorganic nutrients across the six sites

		Net Accumulation Rate					
	Site	C	N	Ca	K	Mg	P
		g m^{-2} yr^{-1}	g m^{-2} yr^{-1}	g m^{-2} yr^{-1}	g m^{-2} yr^{-1}	g m^{-2} yr^{-1}	g m^{-2} yr^{-1}
Year 0 to	Site 1	293 ± 32	16.2 ± 2.2	3.4 ± 0.5	1.29 ± 0.17	0.82 ± 0.11	0.49 ± 0.07
Year 1	Site 2	316 ± 67	13.2 ± 3.5	5.3 ± 1.0	0.87 ± 0.22	0.77 ± 0.20	0.53 ± 0.11
	Site 3	342 ± 53	20.1 ± 3.5	6.6 ± 2.2	1.27 ± 0.15	1.26 ± 0.19	0.74 ± 0.12
	Site 4	139 ± 26	5.7 ± 1.2	2.5 ± 1.4	0.49 ± 0.11	0.64 ± 0.17	0.31 ± 0.13
	Site 5	115 ± 36	6.4 ± 1.5	3.9 ± 1.3	0.37 ± 0.09	0.52 ± 0.11	0.18 ± 0.04
	Site 6	4 ± 1	0.2 ± 0.1	0.2 ± 0.0	0.02 ± 0.00	0.02 ± 0.00	0.01 ± 0.00
Year 1 to	Site 1	129 ± 9	5.3 ± 2.5	2.3 ± 0.2	0.23 ± 0.03	0.29 ± 0.04	0.19 ± 0.02
Year 4	Site 2	94 ± 13	5.9 ± 3.0	3.8 ± 0.3	0.38 ± 0.05	0.45 ± 0.08	0.24 ± 0.04
	Site 3	20 ± 10	1.4 ± 2.5	0.4 ± 0.5	0.06 ± 0.02	0.10 ± 0.04	0.03 ± 0.01
	Site 4	21 ± 8	1.7 ± 0.8	0.2 ± 0.0	0.11 ± 0.01	0.03 ± 0.01	0.02 ± 0.00
	Site 5	28 ± 7	1.6 ± 0.7	1.1 ± 0.4	0.12 ± 0.02	0.13 ± 0.03	0.04 ± 0.01
	Site 6	24 ± 4	1.0 ± 0.6	0.5 ± 0.1	0.08 ± 0.01	0.11 ± 0.02	0.04 ± 0.01
		Retention from Litterfall and Throughfall					
		C	N	Ca	K	Mg	P
		%	%	%	%	%	%
Year 0 to	Site 1	83 ± 11	87 ± 16	77 ± 16	33 ± 7	99 ± 12	96 ± 15
Year 1	Site 2	90 ± 9	67 ± 14	60 ± 12	25 ± 3	51 ± 10	79 ± 6
	Site 3	86 ± 7	81 ± 12	82 ± 13	35 ± 5	74 ± 13	29 ± 12
	Site 4	48 ± 6	34 ± 7	31 ± 6	27 ± 5	63 ± 12	53 ± 9
	Site 5	31 ± 4	33 ± 6	30 ± 5	6 ± 1	27 ± 5	20 ± 3
	Site 6	1 ± 0	1 ± 0	1 ± 0	0.2 ± 0.0	0.4 ± 0.1	1 ± 0
Year 1 to	Site 1	51 ± 10	41 ± 12	60 ± 13	7 ± 1	46 ± 10	77 ± 12
Year 4	Site 2	44 ± 7	48 ± 14	53 ± 11	9 ± 2	46 ± 11	21 ± 4
	Site 3	7 ± 1	8 ± 2	7 ± 1	2 ± 0	8 ± 1	4 ± 1
	Site 4	9 ± 2	13 ± 3	5 ± 1	8 ± 2	5 ± 1	8 ± 1
	Site 5	11 ± 2	10 ± 2	13 ± 2	3 ± 0	10 ± 2	7 ± 1
	Site 6	10 ± 1	7 ± 1	4 ± 1	1 ± 0	4 ± 1	4 ± 1

Rates of accumulation are from Year 0 to 1 and Year 1 to 4 to show changes in accumulation rate with maturation. Retention of Litterfall and Throughfall were calculated using Eq. 1

Root-access and rooting effect on mineral soil C, N, and nutrients

In our question 2, we hypothesized that the presence or biomass of roots in the soil columns could be altered by the presence of the organic horizon and would impact C and nutrient cycling within the mineral soil through enhanced stabilization. Across all 2022 soil columns, root biomass ranged between 48 and 1443 g m^{-2}. Root biomass was significantly lower in root-exclusion than root-access soil columns for all sites using the Kruskal–Wallis test with post-hoc Wilcoxon Rank Sum test. Using LMMs, we found that root biomass within the soil columns was not impacted by MAT across sites in either root-exclusion or root-access soil columns (Fig. 5).

Tree roots were not expected to enter the root-exclusion soil columns from below due to gravitropism, and tree roots did not occur above the bottom mesh in the Year 1 and Year 4 collected columns. However, roots were present in the root-exclusion columns from germinating seedlings and understory plants. Root-access soil columns had significantly higher total root biomass than root-exclusion columns, at ~ 2 × the rate (Fig. 5). The root-exclusion soil columns without access windows had root biomasses ranging between 180 and 480 g m^{-2}, which was significantly less than the

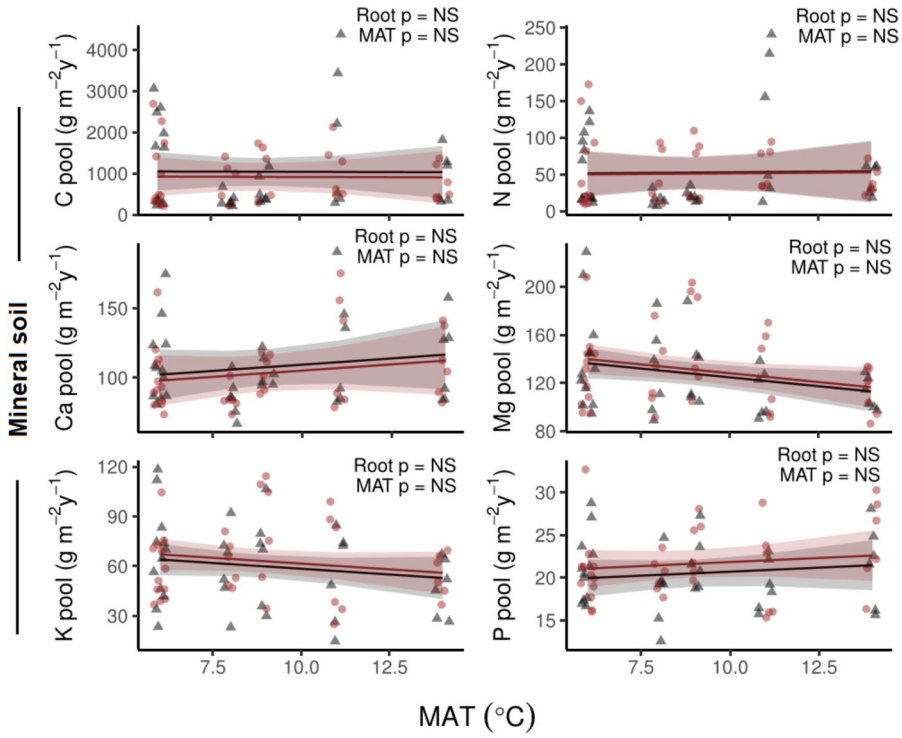

Fig. 4 Mineral soil C and nutrient (N, Ca, Mg, K, P) pools in the soil cores across MAT 30 year averages and separated by root access (red) and root exclusion (black). The predictions are based on a linear mixed-effects model with random effects for replicates nested within site. Continuous lines represent the model's predicted values, and 95% confidence intervals were calculated using the model's estimated variance. Full model results in Supplemental Table 7, random effects in Supplementary Table 9, and alternative models including root biomass in place of root access/exclusion in Supplemental Table 12

root-access soil columns which had root biomass of 707 to 1140 g m^{-2}.

Mineral soil organic particulate and aluminosilicate phases using SEM–EDS

As opposed to using operationally-defined extraction, we imaged elemental maps of Ca, Mg, K, and P within aluminosilicate phases and non- aluminosilicate phases (assumed to be organic particulates due to their lack of spatially-associated aluminosilicate minerals) in the Year 4 mineral soil miniprofiles using SEM–EDS (see Fig. 6). We compared the elemental maps from Year 4 with Year 0 to identify the change in relative proportion within the soil. The fraction of Ca in organic particulate phases increased 13–22% across the six sites, which was significant for Site 1, Site 4, Site 5, and Site 6. The fraction of Mg in organic particulate phases increased 16–24% across the six sites and was significant for all sites except Site 3. The fraction of K in organic particulate phases increased 8–19% across the six sites and was significant for all sites except Site 3. The largest shift in phase occurred for P, 47–64% across the six sites. Furthermore, Site 4 and Site 6 organic particulate P fractions were significantly greater than Site 5. These results agree that with increasing decomposition and mineralization of litter inputs, the mineral soil is accumulating greater organic, non-mineral associated nutrients which is consistent with previous studies on forests (Cotrufo et al 2019).

Discussion

Decreasing C, N, and nutrient accumulation rate with MAT for the organic horizon but not the mineral soil

Our results partially support question 1 hypotheses, showing that organic horizon mass, C, N, and inorganic nutrient pools decreased with MAT along the climate gradient, both one year and four years after the transplanted soils were deployed. Differences in organic horizon C, N, and inorganic nutrient pools were most marked between Sites 1 and 2 to Sites 5 and 6 and also detectable with MAT using a Linear Mixed-effect model. This difference occurred despite comparable litterfall mass inputs and throughfall deposition. Our organic horizon pool data support the general knowledge that organic horizons development

Table 4 Mineral soil mean rate of accumulation rates of C, N, and inorganic nutrients across the six sites

		Net Accumulation Rate					
	Site	C	N	Ca	K	Mg	P
		g m^{-2} yr^{-1}	g m^{-2} yr^{-1}	g m^{-2} yr^{-1}	g m^{-2} yr^{-1}	g m^{-2} yr^{-1}	g m^{-2} yr^{-1}
Year 0 to	Site 1	218 ± 22	12 ± 1	33 ± 9	19 ± 4	18 ± 10	5.6 ± 1.8
Year 1	Site 2	325 ± 35	18 ± 1	42 ± 9	29 ± 5	27 ± 9	7.7 ± 1.6
	Site 3	336 ± 32	18 ± 2	33 ± 7	30 ± 8	27 ± 9	7.5 ± 1.5
	Site 4	336 ± 37	18 ± 2	33 ± 8	30 ± 5	27 ± 8	7.5 ± 2.1
	Site 5	417 ± 48	32 ± 5	24 ± 7	11 ± 5	8 ± 2	3.7 ± 1.5
	Site 6	341 ± 23	25 ± 2	28 ± 7	19 ± 4	10 ± 8	6.9 ± 2.3
Year 1 to	Site 1	408 ± 19	19 ± 4	7 ± 4	15 ± 3	17 ± 5	2.1 ± 0.8
Year 4	Site 2	518 ± 17	29 ± 4	18 ± 5	16 ± 3	19 ± 5	2.8 ± 0.9
	Site 3	285 ± 15	14 ± 4	13 ± 3	19 ± 3	22 ± 4	3.2 ± 1.6
	Site 4	190 ± 14	11 ± 4	6 ± 3	14 ± 2	17 ± 4	2.1 ± 0.5
	Site 5	608 ± 22	36 ± 5	24 ± 4	16 ± 2	14 ± 4	2.7 ± 0.7
	Site 6	307 ± 12	14 ± 2	18 ± 4	11 ± 2	10 ± 3	3.4 ± 0.7
		Litterfall and Throughfall Retained					
		C	N	Ca	K	Mg	P
		%	%	%	%	%	%
Year 0 to	Site 1	120 ± 19	117 ± 14	20 ± 4	28 ± 6	9 ± 3	8 ± 2
Year 1	Site 2	86 ± 11	84 ± 8	26 ± 5	20 ± 4	7 ± 2	24 ± 5
	Site 3	113 ± 13	124 ± 16	23 ± 4	17 ± 6	8 ± 2	13 ± 3
	Site 4	91 ± 12	95 ± 13	17 ± 3	7 ± 2	4 ± 1	6 ± 2
	Site 5	78 ± 10	63 ± 9	59 ± 10	94 ± 19	28 ± 6	31 ± 6
	Site 6	81 ± 7	65 ± 6	82 ± 14	45 ± 11	115 ± 26	27 ± 5
Year 1 to	Site 1	78 ± 8	91 ± 8	71 ± 15	29 ± 6	5 ± 2	18 ± 6
Year 4	Site 2	48 ± 6	51 ± 11	51 ± 12	33 ± 6	7 ± 2	61 ± 26
	Site 3	123 ± 14	116 ± 16	50 ± 8	19 ± 5	7 ± 3	28 ± 8
	Site 4	106 ± 10	121 ± 19	75 ± 13	13 ± 4	5 ± 2	20 ± 6
	Site 5	48 ± 6	50 ± 8	44 ± 7	37 ± 8	12 ± 3	29 ± 5
	Site 6	85 ± 8	110 ± 17	98 ± 17	63 ± 11	36 ± 6	42 ± 9

Rates of accumulation are from Year 0 to 1 and Year 1 to 4 to show changes in accumulation rate with maturation. The %Litterfall and Throughfall retained were calculated using Eq. 2 to evaluate the amount of C, N, and nutrients in the mineral soil that can be attributed to litterfall and throughfall fluxes and not retained in the overlying organic horizon

in temperate forests decreases with increasing MAT (e.g., Binkley and Fisher 2019). While the faster litter decomposition at warmer sites is likely due to higher MAT (Kang et al 2009; Berg and McClaugherty 2020), covarying factors of tree genera and soil invertebrate ecology also likely play a role. The greater organic horizon masses also corresponded with greater inorganic nutrient pools. From Year 0 to Year 1, Site 1 through Site 4 retention of Ca, Mg, and P exhibited a range from 29 up to 99% of the added litterfall and throughfall inputs, which was greater than the 1 up to 30% for Sites 5 and Site 6 (Table 3). Our retention data shows that the organic horizon serves as an important nutrient reservoir at lower MAT sites while the organic horizon at higher MAT sites can be a weak to negligible reservoir for C, N, and nutrients. However, the retention is also element-specific as the highly soluble K had low retention rates across all sites, ranging from 25 to 35% at Sites 1 through 4 and 0.2 to 6% at Sites 5 and 6 (Table 3). Our retention rate data decreased from Year 1 and Year 4 collections, showing that C, N, and inorganic nutrients are retained at lower rates as materials are lost from the organic horizon from leaching, particulate transport, and microbial decomposition and mineralization of C and N compounds.

Our results highlight that there were significant differences in organic horizon development and elemental storage with MAT, particularly between the most northern and southern sites. This climate

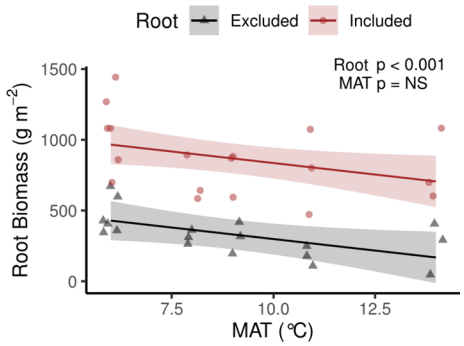

Fig. 5 Mineral soil dry root biomass collected from cores across varying MAT 30 year averages, separated by root-access (red) and root-exclusion (black) in Year 4. The predictions are based on a linear mixed-effects model with random effects for the replicate nested within site. Continuous lines represent the model's predicted values, and 95% confidence intervals were calculated using the model's estimated variance. Model results for random effects are provided in Supplemental Table 9

effect agrees with Berg and McClaugherty (2020) and Bradford et al (2016) in which litter decomposition rates can increase with higher MAT within the temperate forest regime and especially between near subtropical MAT at Site 6 compared with near boreal temperatures at Sites 1 and 2. Organic horizon C and nutrient accumulation was rapid during the first year but had begun to slow down, except at Site 6, which was increasing. Our findings at Sites 1 through 4 disagree with litter decomposition models in which the early stages of organic horizon development are slowest and litter decomposition is most rapid (Berg and McClaugherty 2020). Dozens of litter bag experiments have shown the accumulation of more recalcitrant decomposed litter slows down overall decomposition rates and mass loss, which would promote organic horizon formation (Kang et al 2009; Bradford et al 2016; Berg and McClaugherty 2020). However, our soil columns had only developed Oi and Oe horizons but not Oa horizons. The slow initial decomposition rate could be an artefact of the soil column installation disturbing decomposer communities and their recolonization and access to litter within the soil columns have increased the decomposition rate. As the organic horizon continues to develop, we expect continued accumulation and storage through the formation of organo-mineral SOC.

Our mineral soil results do not support our expected findings of decreased mineral soil C, N, and inorganic nutrientsin question 1. Transplanted mineral soils within the soil columns accumulated C, N, and inorganic nutrients at generally comparable rates across the temperature gradient, except with a few site-specific differences. Using the LMMs to evaluate the effect of temperate, mineral soil C and N did not vary significantly with MAT (Fig. 4, Supplemental Tables S7 and S12) contrary to our hypotheses of increased mineral soil accumulation corresponding with decreased organic horizon development. These results show that MAT did not have a strong effect on the formation of mineral soil pools on C and N following the four years of mineral soil development despite significant difference occurring in the overlying organic horizon. We hypothesize that C and N at the colder sites were stored within the organic horizon while C and N at the warmer sites did not accumulate in the mineral soil due to mineralization instead of formation of stabile SOC or organo-mineral complexes (Kang et al. 2009; Bradford et al. 2016; Berg et al. 1993). Our finding is contrary to our expected mechanisms of faster mineral soil accumulation of C and nutrients within the underlying mineral soil due to higher mean annual temperatures and less organic horizon development. At the higher MAT sites, decomposition may have promoted greater C mineralization of litter (Oi material) by invertebrates preventing the formation of hemified organic matter (Oe material) in the organic horizon or SOC (Oa material) in the mineral soil by microbial cycling (Bradford et al. 2016; Prescott and Vesterdal 2021; Wu et al. 2021). However, our findings do support Sokol et al. (2019) that shoot and litter inputs are less effective ways of forming SOC than roots.

Mineral soil inorganic nutrients pools also did not decrease with MAT. Without decreased SOC and no changes in mineral soil clay content, inorganic nutrients were likely limited in sorption sites (e.g., Gruba and Mulder 2015) or were leached through the mineral soil columns at comparable rates across the temperature gradient. Since mineral soil masses within the columns did not significantly change over the experiment, thus changes in mineral soil accumulation of nutrients were largely driven by changes in elemental concentrations (Supplemental Figure S4). The transplanted material contained only Ca, Mg, K, and P forms that were insoluble under strong acid washes, strong base washes, and resistant to 30% H_2O_2 treatments,

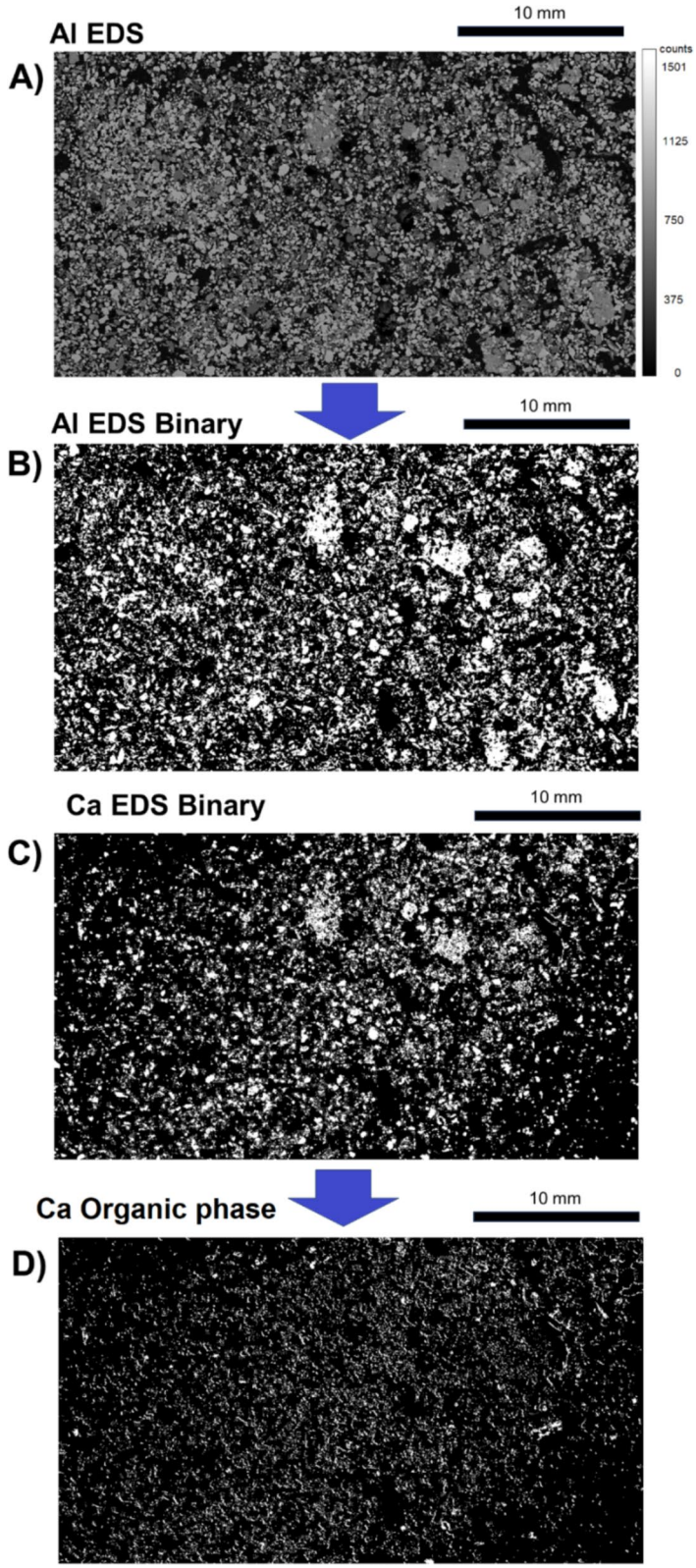

Fig. 6 Conversion of SEM elemental maps to estimates of organic and aluminosilicate phase nutrients is shown. Panel A shows the EDS map of Aluminum for a miniprofile sample for the 2022 soil column samples. Panel B shows the conversion of gray scale EDS to binary by setting a minimum threshold using Image Segmenter in Matlab. Panel C shows the Ca EDS binary for the same Miniprofile sample. Lastly, Panel D is the subtraction of the Al binary from the Ca binary to indicate where Ca is present without Al, indicating non-aluminosilicate phases defined here as organic particulate phase

which most likely were within clay mineral layers. Inorganic nutrient Ca, Mg, K, and P were present in the starting soil material, within muscovite, kaolinite, feldspars, and accessory minerals.

Generally, the results show that mineral soil C and N can be attributed to litterfall but inorganic nutrients such as Ca, K, Mg, and P in litterfall and throughfall could only explain a small fraction of the mineral soil pools. Our measured concentrations for litter were within the range of species-specific tree leaf elemental data assembled by Blinn and Bucker (1989). Moreover, Muller and Martin (1983) and Blinn and Bucker (1989) also observed higher Ca, Mg, K and P also found higher concentrations in hickory and tuliptree than maple and American beech. Although concentrations can show genera specific effects, the total mass of the litterfall flux to the soil columns is more important to understanding inputs to the soil and development of the organic horizon. Across both time periods, inorganic nutrients retained from litterfall and throughfall exhibited a wide variation with no consistent trend across the temperature gradient (Table 4). Across all six sites and both sampling periods, average retention of litterfall and throughfall C and N inputs were between $88\% \pm 13\%$ and $102\% \pm 19\%$, indicating that the majority of C and N in the mineral soil can be attributed to the aboveground inputs. However, across all six sites and from Year 0 to Year 1, average retention of litterfall and throughfall Ca, Mg, K, and P inputs were between $18\% \pm 4\%$ up to $38\% \pm 11\%$, indicating that the majority of inorganic nutrients in the mineral soil cannot be attributed to only aboveground inputs. Our results imply that other processes were important sources of Ca, K, Mg, and P to the transplanted mineral soil columns, which we hypothesize include biotic and abiotic mineral weathering within the transplanted soil material (Séguin et al. 2005), root and mycorrhizal translocation into the soil columns from the native soil (George et al. 1995), vertical and lateral flow of dissolved compounds (Kaiser et al. 2002; Bol et al. 2016; Prakash et al. 2017). These field-based transplant observations of mineral soils show that inorganic nutrient biogeochemistry can be strongly influenced by belowground processes more intensively than aboveground inputs.

Rooting and rooting effects on C, N, and nutrients in the mineral soil decoupled

Our results do not support our expected hypotheses and mechanism for question 2, as we expected rooting to decrease with MAT and significantly decrease mineral soil C, N, and inorganic nutrients due to roots adding SOC to help stabilize additional litterfall inputs but generally this did not occur. Our LMM and Kruskal–Wallis comparisons among the end member sites (Site 1 and 2 compared to Site 5 and 6) showed that root-access did not significantly alter mineral soil nutrient pools (Fig. 4, Supplemental Tables S7 and S12), which leads us to reject our hypothesis of enhanced nutrient pools in the mineral soil increasing due to root abundance. These findings agree with root and litter long-term Detrital Input and Removal Treatment (DIRT) experiment at mixed deciduous-coniferous Oregon forest, in which roots did not increase SOC storage over 20 years (Pierson et al. 2021). However, our finding disagrees with other previous studies investigating SOC formation by roots such as Sokol et al. (2019) and Yang et al. (2023) that found significantly higher C storage with plant rooting. However, their studies focused on C4 grass systems and may not be as applicable to temperate hardwood forests. There are two additional possible explanations for the lack of differences in root-access on mineral soil C, N, and nutrient accumulation in the mineral soil. First, the root abundance effect on mineral soil may not have had enough time to be expressed via mature rhizosphere or been masked by other variables not evaluated in our study. Second, root biomass was comparable across sites, thus rhizodeposition and stabilization of SOC would have been comparable along the temperature gradient (Pierson et al. 2021; Dijkstra et al. 2021).

We examined if organic horizon mass corresponded with greater root biomass in the transplanted soil columns after 4 years of deployment using LMMs (Figs. 3 and 4, Supplemental Tables S6, S7, S11 and S12). Root-access and root biomass were not associated with greater organic horizon C, N, and inorganic nutrient pools, which does not support our hypothesis of an association between the organic horizon and upper mineral soil rooting. Thus, our results either imply that the organic horizon does not promote the preferential rooting in the upper mineral horizons (A and/or Oa horizons) to access nutrients or our

experimental design did not allow us to assess differences in shallow rooting such as the size or number of the transplanted soil columns or rooting differences in genera along the gradient as examples. In particular, only half of the soil columns had root access, decreasing the sample size and statistical power to identify differences along the climate gradient. Further studies focused on woody plant rooting in the organic horizon and underlying mineral soil under laboratory conditions are warranted to evaluate potential synergy.

Limited shifts in inorganic nutrient form in the mineral soil with increasing MAT and roots

For question 3, we expected the proportion of organic particulate phase inorganic nutrients to shift with MAT and root abundance. But using LMMs (Fig. 7, Supplemental Tables S8 and S13), we did not observe a significant difference in the proportion of Ca, Mg, and P in organic particulate phases across the MAT gradient (Fig. 7, Supplemental Tables S8 and S13). The fraction of K in organic phases was significantly higher with root-exclusion than root-access, which is the opposite effect of our hypothesis. We attribute the higher root biomass to increased uptake and removal of organically-bound K. It is important to note that these results differ from the popular measurement of MAOM and particulate organic matter (POM) retention of C and N because those methods are operationally-defined by densities and would lose soluble inorganic nutrients during aqueous separation (e.g., Leuthold et al. 2024). Unfortunately, since C and N cannot be measured by SEM–EDS due to matrix effect, the confirmation of POM cannot be readily confirmed and is based upon the assumption of minerals being well presented by the presence of Al as

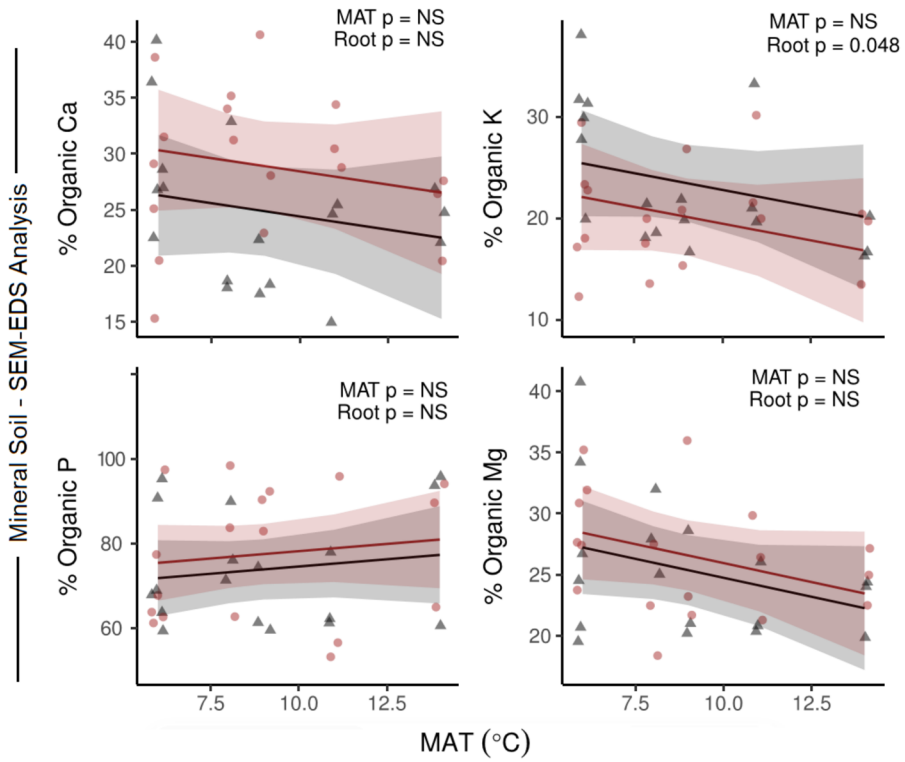

Fig. 7 Change in % organic phases of mineral nutrients (Ca, Mg, K, P) in the cores across varying MAT 30 year averages, separated by root access (red) and exclusion (black). Data represent the difference between % organic phases in cores collected from the field and control media kept in sterile conditions. The predictions are based on a linear mixed-effects model with random effects for the replicate nested within site. Continuous lines represent the model's predicted values, and 95% confidence intervals were calculated using the model's estimated variance. Full model results in Supplemental Table 8, random effects in Supplementary Table 10, and alternative models including root biomass in place of root access/exclusion in Supplemental Table 13

amorphous or crystalline aluminosilicates (e.g., Xiao et al. 2015). Despite these limitations, our results show that particulate fractions of nutrients increased with mineral soil development but differences with MAT were not found.

Study limitations

Our study is one of the first to leverage transplanted materials in field deployment across a large regional gradient in temperate forest ecosystems. Because of the exploratory nature in experimental design, there were several limitations to the study and assessment of C, N, and inorganic nutrient accumulation and retention. A first limitation is that the soil columns were small to be able to deploy 144 columns in total, at 12 root-exclusion and 12 root-access replicates at each of the six sites. Each of the columns required 0.57 kg of washed soil material that was reacted with strong acids, bases, and oxidants to remove as much amorphous minerals, organic matter, and other reactive surfaces from any soil development. Utilizing larger columns would be able to capture more litterfall and throughfall, allow for more root growth, and better avoid microtopographic effects, all of which would reduce the heterogeneity among the soil columns. A second limitation is that soil dwelling organisms were not evaluated in this study. Invertebrates are important decomposers responsible for shredding and translocating leaf litter (Frouz et al. 2015; Prescott and Vesterdal 2021) and their abundance and feeding guilds likely varied across the sites. However, due to their ephemeral nature and limitations on annual sampling trips to the sites, we could not easily and reliably assess their abundance nor evaluate their role in litter decomposition. Similarly, microbial communities' abundance, composition, and physiological traits can shift throughout the growing season (e.g., Craig et al. 2022). A fourth limitation is that the effect of roots on the transplanted mineral soil columns can act to add or remove C, N, and inorganic nutrients. The colonization of the transplanted mineral soil columns may have added C, N, and inorganic nutrients through translocating elements into new growth or enhanced weathering in the rhizosphere (Zhu et al. 2014b; Dotaniya and Meena 2015). Conversely, roots can remove N and inorganic nutrients via root uptake to other aboveground or belowground tissues or stimulate the mineralization of SOC by the priming effect (Panchal et al. 2022; Subramanian et al. 2022). Our study was not designed to separate the individual processes but to examine the net effect on the transplanted mineral soil. Fifth, soil columns are typically considered as 1D downward transport systems (Lewis and Sjöstrom 2010), but the transplanted soil columns likely underwent upward movement during freeze–thaw and high shallow groundwater conditions. Lastly, the transplanted soil columns were analyzed following four years of deployment. As noted by Berg and McClaugherty(2020), these short-term studies are unlikely to capture longer process operating at the decadal to century time scales required for pedogenesis. Despite these limitations, our study has shown that C, N, and inorganic nutrient pools in the organic horizon development do vary with temperature, but mineral soil accumulation did not vary significantly even when controlling soil parent material heterogeneity.

Conclusions

Conclusions from findings

Our central goal was to evaluate the synergistic influence of MAT, rooting, and organic horizon development on the accumulation of C, N, and inorganic nutrients in the organic horizon and transplanted mineral soil columns within six temperate hardwood forests along a latitudinal gradient. For question #1, our results show that C, N, and nutrient accumulation in the organic horizon decreased with increasing MAT. Organic horizon pools were 4 to 5 × greater at the coldest sites than the warmest sites (Fig. 8). Through our litterfall and throughfall monitoring, we can firmly state that the differences in organic horizon pools were not due to differences in input, as Site 5 and Site 6 had comparable or higher inputs compared with the other sites. Thus, the decomposition and mineralization pathway and translocation from the organic horizon was enhanced with increasing MAT. Our findings show that transplanted mineral soil pools of C, N, and inorganic nutrients did not consistently decrease with MAT. On the basis of our mass balance of inputs, the lack of difference in transplanted mineral soil C, N, and inorganic nutrients cannot be attributed to differences in organic horizon accumulation.

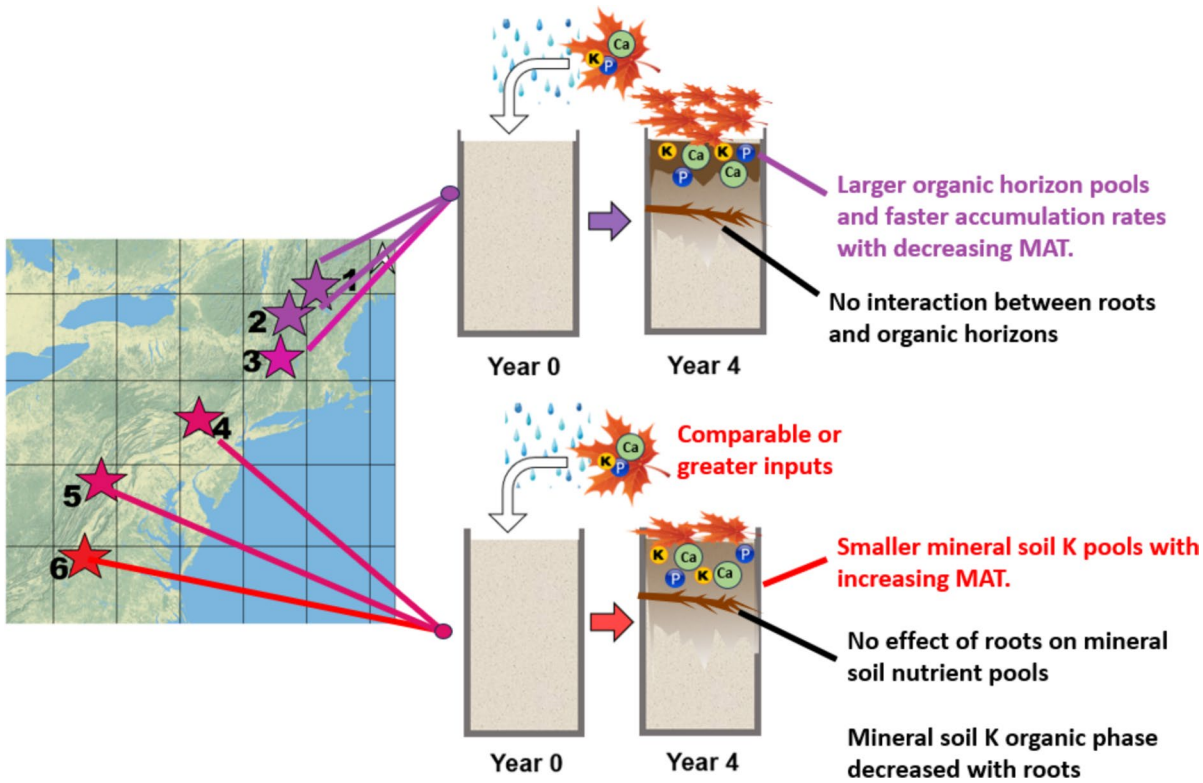

Fig. 8 Conceptual figure of the main findings of our study, illustrating larger organic horizon pools and faster nutrient accumulation rates with decreasing MAT, only smaller mineral soil K pools with increasing MAT, no interaction between roots and the organic horizon, and no effect of root access on mineral soil pools

Differences may not have arisen due to the short duration of only 4 years or have been masked by the limitations discussed in Sect. "Study limitations".

For question #2, we did not find evidence of significantly greater root biomass with lower MAT nor greater stabilization of C, N, and nutrients in the mineral soil. Root biomass was 2 × greater in root-exclusion (707–1140 g m^{-2}) than root-access (180–480 g m^{-2}) soil columns. Total root biomass was not associated with organic horizon size or nutrient pools, which does not support our hypothesis that organic horizon development would stimulate upper mineral soil rooting for nutrients. Furthermore, our mineral soil findings did not find a consistent association between total root biomass with mineral soil nutrient C, N, and inorganic nutrient pools. A root priming effect or root-uptake effect may not have had enough time to develop or been masked by heterogeneity in tree genera, organic horizon development rates, or other variables not evaluated in this study such as invertebrate scavengers and microbial communities.

In our last question #3, we found that inorganic nutrients organic particulate phases increased in the transplanted mineral soil across all six sites using SEM–EDS imaging from Year 0 to Year 4. However, we did not find a significant effect of MAT or site-specific differences in the organic particulate phase nutrients. With the exception of higher organic K particulate phase in root-exclusion columns, we did not find an effect of root-access on particulate phase Ca, Mg, or P. Thus root access and MAT did not increase the particulate phase of the inorganic nutrients over the relatively short duration of the experiment. We look forward to the next collection of transplanted soil columns across these six sites to shed light on if additional time will show significant changes or continue to support these earlier findings.

Acknowledgements We thank Dr. Ashley Keiser, William Caston, Ainsley McStay, and several additional UMass Amherst students for helping sort and identify tree litter. We also thank Dartmouth College, Smith College, Vermont Department of Forests, Parks, and Recreation, Pennsylvania Bureau of Forestry, and Virginia Department of Forestry for permitting research activities and site access.

Author contributions Conceptualization J.R., A.D.; methodology J.R., A.D.; writing—original draft preparation, J.R.; writing—review and editing, J.R., A.D.; statistical analyses and visualization, A.D., J.R.; funding acquisition, J.R. A.D.

Funding This work was supported by was funded by the U.S. National Science Foundation Award Number: 2052046 to P.I. Justin Richardson and Co-I Annise M. Dobson and the University of Massachusetts Amherst with funding to PI Justin Richardson.

Data availability Datasets generated for this study are available within the supplementary material.

Declarations

Competing interests Justin Richardson and Annise Dobson declare they have no financial interests and have no relevant financial or non-financial interests to disclose.

References

Adams MB, Kelly C, Kabrick J, Schuler J (2019) Temperate forests and soils. Dev Soil Sci 36:83–108

Augusto L, Ranger J, Binkley D, Rothe A (2002) Impact of several common tree species of European temperate forests on soil fertility. Ann for Sci 59(3):233–253

Barton K (2023) MuMIn: multi-model inference. R package version 1.47.1. https://CRAN.R-project.org/package=MuMIn

Berg B, Berg MP, Bottner P, Box E, Breymeyer A, De Anta RC, Couteaux M, Escudero A, Gallardo A, Kratz W, Madeira M (1993) Litter mass loss rates in pine forests of Europe and Eastern United States: some relationships with climate and litter quality. Biogeochemistry 20:127–159

Berg B, McClaugherty C (2020) Climate Gradients. Substrate quality versus climate and their interactions. Plant litter: decomposition, humus formation, carbon sequestration, pp 165–187

Binkley D, Fisher RF (2019) Ecology and management of forest soils. John Wiley & Sons

Blinn CR, Bucker ER (1989) Normal foliar nutrient levels in North American forest trees. Minnesota Agricultural Experiment Station; University of Minnesota. Station Bulletin 590

Bol R, Julich D, Brödlin D, Siemens J, Kaiser K, Dippold MA, Spielvogel S, Zilla T, Mewes D, von Blanckenburg F, Puhlmann H (2016) Dissolved and colloidal phosphorus fluxes in forest ecosystems—an almost blind spot in ecosystem research. J Plant Nutr Soil Sci 179(4):425–438

Bowden RD, Simpson MJ, Saucedo NP, Brozell K, DiGiacomo J, Lajtha K (2024) Litter and root sources of soil organic matter in a temperate forest: thirty years in the DIRT. Soil Sci Soc Am J. https://doi.org/10.1002/saj2.20634

Bradford MA, Berg B, Maynard DS, Wieder WR, Wood SA (2016) Understanding the dominant controls on litter decomposition. J Ecol 104:229–238

Brandt AJ, del Pino GA, Burns JH (2014) Experimental protocol for manipulating plant-induced soil heterogeneity. J Visual Exp 85:e51580

Ciolkosz EJ, Carter BJ, Hoover MT, Cronce RC, Waltman WJ, Dobos RR (1990) Genesis of soils and landscapes in the Ridge and Valley province of central Pennsylvania. Geomorphology 3(3-4):245–261.

Chauhan RP, Nain M, Kant K (2008) Radon diffusion studies through some building materials: effect of grain size. Radiat Meas 43:S445–S448

Chen M, Ma LQ (2001) Comparison of three aqua regia digestion methods for twenty Florida soils. Soil Sci Soc Am J 65(2):491–499

Cotrufo MF, Ranalli MG, Haddix ML, Six J, Lugato E (2019) Soil carbon storage informed by particulate and mineral-associated organic matter. Nat Geosci 12(12):989–994

Craig ME, Geyer KM, Beidler KV, Brzostek ER, Frey SD, Stuart Grandy A, Liang C, Phillips RP (2022) Fast-decaying plant litter enhances soil carbon in temperate forests but not through microbial physiological traits. Nat Commun 13(1):1229

Dhillon GS, Amichev BY, De Freitas R, Van Rees K (2015) Accurate and precise measurement of organic carbon content in carbonate-rich soils. Commun Soil Sci Plant Anal 46(21):2707–2720

Dijkstra FA, Zhu B, Cheng W (2021) Root effects on soil organic carbon: a double-edged sword. New Phytol 230(1):60–65

Dotaniya ML, Meena VD (2015) Rhizosphere effect on nutrient availability in soil and its uptake by plants: a review. Proc Natl Acad Sci India Sect B Biol Sci 85:1–12

Eberl DD (2004) Quantitative mineralogy of the Yukon River system: changes with reach and season, and determining sediment provenance. Am Mineral 89:1784–1794

Frouz J, Roubíčková A, Heděnec P, Tajovský K (2015) Do soil fauna really hasten litter decomposition? A meta-analysis of enclosure studies. Eur J Soil Biol 68:18–24

Gao G, Liu Z, Wang Y, Wang S, Ju C, Gu J (2021) Tamm review: fine root biomass in the organic (O) horizon in forest ecosystems: global patterns and controlling factors. For Ecol Manage 491:119208

George E, Marschner H, Jakobsen I (1995) Role of arbuscular mycorrhizal fungi in uptake of phosphorus and nitrogen from soil. Crit Rev Biotechnol 15(3–4):257–270

Gosz JR, Likens GE, Bormann FH (1972) Nutrient content of litter fall on the Hubbard Brook experimental forest, New Hampshire. Ecology 53(5):769–784

Gruba P, Mulder J (2015) Tree species affect cation exchange capacity (CEC) and cation binding properties of organic matter in acid forest soils. Sci Total Environ 511:655–662

Hagen-Thorn A, Callesen I, Armolaitis K, Nihlgård B (2004) The impact of six European tree species on the chemistry of mineral topsoil in forest plantations on former agricultural land. For Ecol Manage 195(3):373–384

Heděnec P, Zheng H, Siqueira DP, Peng Y, Schmidt IK, Frøslev TG, Kjøller R, Li H, Frouz J, Vesterdal L (2023) Litter chemistry of common European tree species drives the feeding preference and consumption rate of soil invertebrates, and shapes the diversity and structure of gut and faecal microbiomes. Soil Biol Biochem 177:108918

Hobbie SE (2015) Plant species effects on nutrient cycling: revisiting litter feedbacks. Trends Ecol Evol 30(6):357–363

Huang J, Hartemink AE (2020) Soil and environmental issues in sandy soils. Earth-Sci Rev 208:103295

Jelinski NA, Richardson JB, Nater E (2023) Soils of humid cool temperate regions. Encyclopedia of soils in the environment, Vol 1–5, 2nd edn. Elsevier, pp 4–289

Jones DL, Brassington DS (1998) Sorption of organic acids in acid soils and its implications in the rhizosphere. Eur J Soil Sci 49(3):447–455

Kaiser K, Guggenberger G, Haumaier L, Zech W (2002) The composition of dissolved organic matter in forest soil solutions: changes induced by seasons and passage through the mineral soil. Organic Geochem 33(3):307–318

Kang H, Berg B, Liu C, Westman CJ (2009) Variation in mass-loss rate of foliar litter in relation to climate and litter quality in Eurasian forests: differences among functional groups of litter. Silva Fenn 43(4):549–575

Kaplan S, Ropelewska E, Günaydın S, Sabancı K, Çetin N (2024) Machine learning and computer vision technology to analyze and discriminate soil samples. Sci Rep 14(1):19945

Keeton WS (2006) Managing for late-successional/old-growth characteristics in northern hardwood-conifer forests. For Ecol Manage 235(1–3):129–142

Kome GK, Enang RK, Tabi FO, Yerima BPK (2019) Influence of clay minerals on some soil fertility attributes: a review. Open Journal of Soil Science 9(9):155–188

Kooijman AM, Weiler HA, Cusell C, Anders N, Meng X, Seijmonsbergen AC, Cammeraat LH (2019) Litter quality and microtopography as key drivers to topsoil properties and understorey plant diversity in ancient broadleaved forests on decalcified marl. Sci Total Environ 684:113–125

Küsel K, Drake HL (1998) Microbial turnover of low molecular weight organic acids during leaf litter decomposition. Soil Biol Biochem 31(1):107–118

Kuznetsova A, Brockhoff PB, Christensen RHB (2017) LmerTest package: tests in linear mixed effects models. J Stat Softw 82(13):1–26. https://doi.org/10.18637/jss.v082.i13

Lang AK, Pett-Ridge J, McFarlane KJ, Phillips RP (2023) Climate, soil mineralogy and mycorrhizal fungi influence soil organic matter fractions in eastern US temperate forests. J Ecol 111(6):1254–1269

Leuthold S, Lavallee JM, Haddix ML, Cotrufo MF (2024) Contrasting properties of soil organic matter fractions isolated by different physical separation methodologies. Geoderma 445:116870

Lewis J, Sjöstrom J (2010) Optimizing the experimental design of soil columns in saturated and unsaturated transport experiments. J Contam Hydrol 115(1–4):1–13

Liu B, Han F, Ning P, Li H, Rengel Z (2022) Root traits and soil nutrient and carbon availability drive soil microbial diversity and composition in a northern temperate forest. Plant Soil 479(1):281–299

Lüdecke, D. (2021). ggeffects: Tidy data frames of marginal effects for 'ggplot'. R package version 1.1.1. https://CRAN.R-project.org/package=ggeffects

Martín-García JM, Márquez R, Delgado G, Sánchez-Marañón M, Delgado R (2015) Relationships between quartz weathering and soil type (Entisol, Inceptisol and Alfisol) in Sierra Nevada (southeast Spain). Eur J Soil Sci 66(1):179–193

McClaugherty CA, Pastor J, Aber JD, Melillo JM (1985) Forest litter decomposition in relation to soil nitrogen dynamics and litter quality. Ecology 66(1):266–275

McEvoy TJ, Sharik TL et al (1980) Vegetative structure of an Appalachian oak forest in southwestern Virginia. Am Midland Naturalist: 96–105

Medhurst J, Parsby JAN, Linder S, Wallin G, Ceschia E, Slaney M (2006) A whole-tree chamber system for examining tree-level physiological responses of field-grown trees to environmental variation and climate change. Plant Cell Environ 29(9):1853–1869

Melillo JM, Richmond TT, Yohe G (2014) Climate change impacts in the United States. Third Nat Clim Assess 52:150–174

Muller RN, Martin WH (1983) Autumn leaf fall and nutrient return in an old-growth and a second-growth forest in eastern Kentucky. Botanical Gazette 144(4):552–558

Neira J, Ortiz M, Morales L, Acevedo E (2015) Oxygen diffusion in soils: understanding the factors and processes needed for modeling. Chil J Agric Res 75:35–44

O'Donnell JA, Aiken GR, Butler KD, Guillemette F, Podgorski DC, Spencer RG (2016) DOM composition and transformation in boreal forest soils: the effects of temperature and organic-horizon decomposition state. J Geophys Res Biogeosciences 121(10):2727–2744

Ott NF, Watmough SA (2021) Contrasting litter nutrient and metal inputs and soil chemistry among five common Eastern North American tree species. Forests 12(5):613

Ouchiyama N, Tanaka T (1986) Porosity estimation from particle size distribution. Ind Eng Chem Fundam 25(1):125–129

Panchal P, Preece C, Peñuelas J, Giri J (2022) Soil carbon sequestration by root exudates. Trends Plant Sci 27(8):749–757

Pierson D, Evans L, Kayhani K, Bowden RD, Nadelhoffer K, Simpson M, Lajtha K (2021) Mineral stabilization of soil carbon is suppressed by live roots, outweighing influences from litter quality or quantity. Biogeochemistry 154(3):433–449

Pietsch KA, Ogle K, Cornelissen JH, Cornwell WK, Bönisch G, Craine JM, Jackson BG, Kattge J, Peltzer DA, Penuelas J, Reich PB (2014) Global relationship of wood and leaf litter decomposability: the role of functional traits within and across plant organs. Glob Ecol Biogeogr 23(9):1046–1057

Prakash D, Benbi DK, Saroa GS (2017) Clay, organic carbon, available P and calcium carbonate effects on phosphorus release and sorption–desorption kinetics in alluvial soils. Commun Soil Sci Plant Anal 48(1):92–106

Prescott CE, Vesterdal L (2021) Decomposition and transformations along the continuum from litter to soil organic matter in forest soils. For Ecol Manage 498:119522

Pretzsch H, del Río M, Biber P, Arcangeli C, Bielak K, Brang P, Dudzinska M, Forrester DI, Klädtke J, Kohnle U, Ledermann T (2019) Maintenance of long-term experiments for unique insights into forest growth dynamics and trends: review and perspectives. Eur J Forest Res 138:165–185

Prietzel J, Klysubun W, Hurtarte LCC (2021) The fate of calcium in temperate forest soils: a Ca K-edge XANES study. Biogeochemistry 152:195–222

PRISM Climate Group (2023) PRISM climate data 4 km 30 year normal data. Oregon State University

Qiu H, Ge T, Liu J, Chen X, Hu Y, Wu J, Su Y, Kuzyakov Y (2018) Effects of biotic and abiotic factors on soil organic matter mineralization: experiments and structural modeling analysis. Eur J Soil Biol 84:27–34

R Core Team (2024) R: A language and environment for statistical computing. R Foundation for Statistical Computing, Vienna

Rasmussen C, Heckman K, Wieder WR, Keiluweit M, Lawrence CR, Berhe AA, Blankinship JC, Crow SE, Druhan JL, Hicks Pries CE, Marin-Spiotta E (2018) Beyond clay: towards an improved set of variables for predicting soil organic matter content. Biogeochemistry 137:297–306

Richardson, J, Dobson A (2024) Litterfall and throughfall data for six sites along Appalachian Mountain Range, Eastern United States. University of Virginia Dataverse, V1. https://doi.org/10.18130/V3/I00LKH

Richardson JB, Friedland AJ (2016) Influence of coniferous and deciduous vegetation on major and trace metals in forests of northern New England, USA. Plant Soil 402(1):363–378

Rouifed S, Handa IT, David JF, Hättenschwiler S (2010) The importance of biotic factors in predicting global change effects on decomposition of temperate forest leaf litter. Oecologia 163:247–256

Schindlbacher A, Zechmeister-Boltenstern S, Butterbach-Bahl K (2004) Effects of soil moisture and temperature on NO, NO2, and N2O emissions from European forest soils. J Geophys Res Atmos. https://doi.org/10.1029/2004JD004590

Scott NA, Cole CV, Elliott ET, Huffman SA (1996) Soil textural control on decomposition and soil organic matter dynamics. Soil Sci Soc Am J 60(4):1102–1109

Séguin V, Courchesne F, Gagnon C, Martin RR, Naftel SJ, Skinner W (2005) Mineral weathering in the rhizosphere of forested soils. Biogeochemistry of trace elements in the rhizosphere. Elsevier, pp 29–55

Šimanský V, Juriga M, Jonczak J, Uzarowicz Ł, Stępień W (2019) How relationships between soil organic matter parameters and soil structure characteristics are affected by the long-term fertilization of a sandy soil. Geoderma 342:75–84

Sokol NW, Kuebbing SE, Karlsen-Ayala E, Bradford MA (2019) Evidence for the primacy of living root inputs, not root or shoot litter, in forming soil organic carbon. New Phytol 221(1):233–246

Stoops G (2021) Guidelines for analysis and description of soil and regolith thin sections, vol 184. John Wiley & Sons

Street BB, Rice AM, Richardson JB (2023) Forest floor and Na azide effect on elements in leachate from contrasting New Hampshire and Virginia forest soils. Soil Sci Soc Am J 87(6):1444–1457

Subramanian D, Subha R, Murugesan AK (2022) Accumulation and translocation of trace elements and macronutrients in different plant species across five study sites. Ecol Indic 135:108522

Sudarsan B, Ji W, Biswas A, Adamchuk V (2016) Microscope-based computer vision to characterize soil texture and soil organic matter. Biosyst Eng 152:41–50

Van Stan JT, Levia DF Jr, Inamdar SP, Lepori-Bui M, Mitchell MJ (2012) The effects of phenoseason and storm characteristics on throughfall solute washoff and leaching dynamics from a temperate deciduous forest canopy. Sci Total Environ 430:48–58

Wang S, Ji H, Ouyang Z, Zhou D, Zhen L, Li T (1999) Preliminary study on weathering and pedogenesis of carbonate rock. Sci China Ser D: Earth Sci 42(6):572–581

Wang Q, Yuan Y, Zhang Z, Liu D, Xiao J, Yin H (2021) Exudate components mediate soil C dynamic through different priming mechanisms in forest soils. Appl Soil Ecol 160:103855

Wu X, Niklas KJ, Sun S (2021) Climate change affects detritus decomposition rates by modifying arthropod performance and species interactions. Curr Opin Insect Sci 47:62–66

Wu Y, Peng Z, Wang X, Huang J, Yang L, Liu L (2025) Warmer climate reduces the carbon storage, stability and saturation levels in forest soils. Earths Future 13(2):e2024EF004988

Xiao J, Wen Y, Li H, Hao J, Shen Q, Ran W, Mei X, He X, Yu G (2015) In situ visualisation and characterisation of the capacity of highly reactive minerals to preserve soil organic matter (SOM) in colloids at submicron scale. Chemosphere 138:225–232

Yang X, Wang B, Fakher A, An S, Kuzyakov Y (2023) Contribution of roots to soil organic carbon: From growth to decomposition experiment. Catena 231:107317

Zani D, Crowther TW, Mo L, Renner SS, Zohner CM (2020) Increased growing-season productivity drives earlier autumn leaf senescence in temperate trees. Science 370(6520):1066–1071

Zhang Y, Hartemink AE, Vanwalleghem T, Bonfatti BR, Moen S (2024) Climate and land use changes explain variation in the A horizon and soil thickness in the United States. Commun Earth Environ 5(1):129

Zhao Z, Wu F, Peng Y, Wu Q, Heděnec P, An N, Yue K (2023) Changes in rainfall pH after passing through the forest canopy: increase in throughfall but decrease in stemflow. J Hydrol 624:129955

Zhu Y, Duan G, Chen B, Peng X, Chen Z, Sun G (2014a) Mineral weathering and element cycling in soil-microorganism-plant system. Sci China Earth Sci 57:888–896

Zhu B, Gutknecht JL, Herman DJ, Keck DC, Firestone MK, Cheng W (2014b) Rhizosphere priming effects on soil carbon and nitrogen mineralization. Soil Biol Biochem 76:183–192

Zukswert JM (2013) Effects of eastern hemlock removal on nutrient cycling and forest ecosystem processes at the MacLeish Field Station, Whately. Undergraduate Thesis. Smith College 130 pp